



REPUBLIC OF TURKEY
ACIBADEM MEHMET ALİ AYDINLAR UNIVERSITY
INSTITUTE OF HEALTH SCIENCES

**TENDON TISSUE ENGINEERING APPROACH USING
GUIDED PLATFORMS AND MESENCHYMAL STEM
CELLS**

TUĞÇE DEVECİ
MASTER THESIS

DEPARTMENT of MEDICAL BIOTECHNOLOGY

SUPERVISOR
Assist. Prof. Dr. Deniz Yücel

ISTANBUL-2020

DECLARATION

I hereby declare that this thesis has been written by me based on the data obtained in line with the academic rules and ethical conduct. I also declare that, as required by these rules and conduct, all the information, data, comments, and analysis have been collected and processed through scientific writing style. Literature has been referenced original sources in accordance with the publication ethics. I announced and emphasize that there is no violation of patent and copyright rights during the study and writing of this thesis.

27/7/2020

Tuğçe DEVECİ



ACKNOWLEDGEMENTS

I would like to express my deepest gratitude to my supervisor Assist. Prof. Dr. Deniz YÜCEL for her continuous guidance, advice, support, encouragement, and insight throughout the research.

I am especially grateful to Prof. Dr. Vasıf HASIRCI for his valuable advices and comments.

I would like to express my sincere gratitude to Prof. Dr. Gamze TORUN KÖSE for her help in chondrogenic differentiation experiments and for her suggestions.

I would like to thank to Hazal GEZMİŞ for helping me in electrospinning studies and in learning cell culture experiments.

I would like to especially thank to Selçuk BİRDOĞAN for his help in scanning electron microscopy.

I would like to thank to Funda CAN and Serap FİDE for helping me to perform mechanical test analysis and their support.

I am grateful to my special lab partners and friends Gözde Ervin KÖLE and Aslıhan AKALINLI for always being with me and their continuous support. We have good memories and good relationship.

I would like to thank to my best friends Hande ÇELİK for her continuous motivation and support.

I would like to thank to the members of ACU Research Laboratory group Nesteren MANSUR, Tayyip KARAMAN, Ayşegül EKMEKÇİOĞLU, Baki KILIÇ, Gülin BARAN, Simge ŞENAY, and my labmates Deniz BAŞÖZ and our technician Görkem GÜN for their support in this study.

I would like to thank to my fiance İsmail Berkay ACUNER for his understanding, helping, and trusting in me.

Finally, I would like to express my deepest gratitude's to my parents Aynur DEVECİ and Engin DEVECİ for their understanding, endless help and support, their patience and trusting in me, not only during this study, but for all my life. I would like to express special thanks to my sister Işıl DEVECİ. I would also like to thank to other members of my family, my grandmother, grandfather, aunts, and cousin Pelin DEVECİ and Mina TOPRAK for their support and encouragement.

This study was supported by Acıbadem Mehmet Ali Aydınlar University ABAPKO (No:2018/01/13), and by TÜBİTAK BİDEB 2210-C Programme (2018-1), and these grants are gratefully acknowledged. I would like to thank METU-BIOMATEN for its physical and technical contribution during my thesis.

TABLE OF CONTENTS

DECLARATION.....	iii
ACKNOWLEDGEMENTS.....	iv
TABLE OF CONTENTS.....	vi
LIST OF ABBREVIATIONS and SYMBOLS.....	x
LIST OF FIGURES.....	xi
LIST OF TABLES.....	xiv
SUMMARY.....	1
ÖZET.....	2
1. BACKGROUND and AIM OF THE STUDY.....	3
2. INTRODUCTION.....	4
2.1 Tendon Tissue.....	4
2.2 Tendon Damages.....	6
2.3 Treatment Methods of Tendon Injuries.....	7
2.4 Tendon Tissue Engineering.....	9
2.4.1 Cell Sources.....	10
2.4.1.1 Mesenchymal Stem Cells.....	12
2.4.2 Scaffolds for Tendon Tissue Engineering.....	14
2.4.2.1 Natural Scaffolds.....	15
2.4.2.2 Synthetic Scaffolds.....	15
2.4.3 Fabrication of Guided Platforms via Electrospinning.....	16
2.4.4 Bioactive Agents.....	20

3. MATERIALS and METHODS.....	21
3.1 Materials	21
3.2 Methods.....	22
3.2.1 Preparation of Scaffolds.....	23
3.2.1.1 Fabrication of Electrospun Fibrous Mats.....	23
3.2.1.2 Morphology Analysis of the Scaffolds by Scanning Electron Microscopy.....	27
3.2.1.3 Mechanical Analysis of the Polymeric Scaffolds.....	27
3.2.2 <i>In Vitro</i> Studies.....	28
3.2.2.1 Isolation and Culture of Human Dental Pulp Mesenchymal Stem Cells.....	28
3.2.2.2 Characterization of Dental Pulp MSCs.....	28
3.2.2.2.1 Morphology Analysis of DP MSCs.....	28
3.2.2.2.2 Growth Kinetics of Dental Pulp MSCs.....	29
3.2.2.2.3 Flow Cytometry Analysis.....	30
3.2.2.2.4 Osteogenic Differentiation of Dental Pulp MSCs.....	30
3.2.2.2.5 Chondrogenic Differentiation of Dental Pulp MSCs.....	32
3.2.2.3 Tenogenic Differentiation of Dental Pulp MSCs.....	32
3.2.2.4 Behaviour of Stem Cells on Electrospun Fibrous Mats.....	33
3.2.2.4.1 Cell Seeding on Electrospun Fibrous Mats.....	33
3.2.2.4.2 DP MSC Organization on the Scaffolds.....	34
3.2.2.4.3 Proliferation and Cell Activity of Cells on Scaffolds.....	34
3.2.2.4.4 Evaluation of tenogenic differentiation of DP MSC on the scaffolds by Immunocytochemistry	35

4. RESULTS.....	36
4.1 Characterization of Electrospun Mats	36
4.1.1 Morphology and Dimension Analysis of the Electrospun Fibrous Mats	36
4.1.2 Mechanical Analysis of the Polymeric Scaffolds.....	40
4.2 <i>In Vitro</i> Studies.....	41
4.2.1 Culture and characterization of Human Dental Pulp MSCs... ..	41
4.2.1.1 Evaluation of DP MSCs Morphology.....	41
4.2.1.2 Growth Kinetics of Dental Pulp MSC.....	43
4.2.1.3 Flow Cytometry Analysis.....	44
4.2.1.4 Osteogenic Differentiation of Dental Pulp MSCs.....	45
4.2.1.5 Chondrogenic Differentiation of Dental Pulp MSCs.....	47
4.2.2 Tenogenic Differentiation of Dental Pulp MSCs.....	49
4.2.3 Behaviour of Stem Cells on Electrospun Fibrous Mats.....	51
4.2.3.1 DP MSC Organization on the Scaffolds.....	51
4.2.3.2 Proliferation and Cell Activity of DP MSCs on the Scaffolds	54
4.2.3.3 Evaluation of Tenogenic Differentiation of DP MSCs on The scaffolds by Immunocytochemistry.....	56
5. DISCUSSION and CONCLUSION.....	65
6. REFERENCES.....	68
7. APPENDICES.....	73
Appendix 1. Calibration curve of human dental pulp mesenchymal stem cells at passage.....	73

Appendix 2. Ethical approval for the use of human DP MSCs.....74
Appendix 3. Ethical approval for the use of human DP MSCs (Continued
Appendix 2)75
CURRICULUM VITAE76



LIST OF ABBREVIATIONS and SYMBOLS

AFM	Aligned Fibrous Mat
ALP	Alkaline Phosphatase
BSA	Bovine Serum Albumin
DMEM	Dulbecco's Modified Eagle Medium
DMSO	Dimethyl Sulfoxide
DP	Dental Pulp
ECM	Extracellular Matrix
FBS	Fetal Bovine Serum
GDF7/BMP12	Growth Differentiation Factor 7 / Bone Morphogenic Protein 12
MSCs	Mesenchymal Stem Cells
PBS	Phosphate Buffer Saline
Pen/Strep	Penicillin/Streptomycin
PEG	Polyethylene Glycol
PFA	Paraformaldehyde
PLGA	Poly(D,L-lactide-co-glycolide)
P(L-D,L)LA	Poly(L-lactide-co-D,L-lactide)
RFM	Random Fibrous Mat
Scx	Scleraxis
TCPs	Tissue Culture Polystyrene
Tnm	Tenomodulin

LIST OF FIGURES

Figure 1. (a) Anatomical structure and (b) organization of tendon tissue.....	5
Figure 2. Different core suture techniques for tendon surgery	8
Figure 3. Principles of tissue engineering	9
Figure 4. Classification of stem cells	11
Figure 5. Multiple differentiation potential of mesenchymal stem cells for repair of various tissues.	13
Figure 6. Schematic illustrations of fiber-production techniques used for scaffolds in tendon tissue engineering. (a) electrospinning of random fibers, (b) electrospinning of aligned fibers, (c) knitting, (d) braiding, (e) E-jetting (f) extrusion, (g) wet spinning and (h)microfiber melt drawing.	17
Figure 7. Chemical structure of melatonin.....	20
Figure 8. Experimental design of the study.....	22
Figure 9. Schematic illustration of electrospinning system to fabricate (a) random fibrous mat and (b) aligned fibrous mat.	24
Figure 10. SEM images of P(L-D,L)LA-PLGA electrospun fibers in the absence of melatonin. (a,b,c) Aligned fibrous mat and (d,e,f) random fibrous mat. Magnifications: (a,d) 350X, scale bar: 400 μ m , (b, e) 2500X, scale bar: 50 μ m, (c, f) 5000X, scale bar: 20 μ m.	37
Figure 11. SEM images of P(L-D,L)LA-PLGA electrospun fibers with melatonin group. (a,b,c) Aligned fibrous mat and (d,e,f) random fibrous mat. Magnifications: (a,d) 350X, scale bar: 400 μ m , (b,e) 2500X, scale bar: 50 μ m, (c,f) 5000X, scale bar: 20 μ m	38
Figure 12. The distribution of fiber diameter of the random fibrous mat	39
Figure 13. The distribution of fiber diameter of the aligned fibrous mat.....	39
Figure 14. Representative stress-strain curve of tensile test of the polymeric films.	40
Figure 15. Light microscope images of human DP MSCs (P3). Magnifications: (a) 4X, (b) 10X, (c) 20X, , (d) 40X	42
Figure 16. Confocal microscope image of DP MSCs (P3) which were stained with Phalloidin-DAPI for actin filaments (green) and nucleus (blue), respectively. Magnification: 20X, scale bar: 50 μ m.	43
Figure 17. Growth kinetics of human DP MSCs (doubling time: 15 \pm 0.3 h)	44

Figure 18. Specific ALP activity of DP MSCs on 14th and 21st days of osteogenic differentiation.....	46
Figure 19. Light microscope images of DP MSCs induced to osteogenic differentiation and undifferentiated cells after von Kossa staining on days 14 and 21. Magnification: X20, scale bar: 50 μ m.	47
Figure 20. Light microscope images of DP MSCs in undifferentiated state and after chondrogenic induction on days 14 and 21 after Alcian Blue staining. Magnification: X10, scale bar: 100 μ m.	48
Figure 21. Confocal images of (a,c) undifferentiated DP MSCs and (b,d) DP MSCs cultured for 14 days in tenogenic induction medium. The expression of tenogenic markers, (a,b) scleraxis (green) and (c,d) tenomodulin (green) were shown by immunocytochemistry. The nucleus (blue) of the cells were counterstained with DAPI Magnification: 20X, scale bar: 50 μ m	50
Figure 22. Confocal microscope images of DP MSCs on the random fibrous mat. The cells were stained with Phalloidin-DAPI for actin filaments (green) and nuclues (blue), respectively. Magnification: a) 20X, scale bar: 50 μ m, b) 40X, scale bar: 20 μ m.	52
Figure 23. Confocal microscope images of DP MSCs on the aligned electrospun fibrous mat. The cells were stained with Phalloidin-DAPI for actin filaments (green) and nuclues (blue), respectively. Magnification: a) 20X, scale bar: 50 μ m, b) 40X, scale bar: 20 μ m.	53
Figure 24. Proliferation of DP MSCs on P(L-D,L)LA-PLGA electrospun fibrous mats prepared in the absence of melatonin (without melatonin group).	55
Figure 25. Proliferation of DP MSCs on P(L-D,L)LA-PLGA electrospun fibrous mat in the presence of melatonin (with melatonin group)	55
Figure 26. Confocal images of the cells on the aligned fibrous mat with melatonin at the end of 14 day of tenogenic induction. The cells were immunostained against scleraxis (green) and counterstained with DAPI for nucleus (blue). Magnifications: (a) X20, scale bar: 50 μ m, (b) X40, scale bar: 20 μ m.....	57
Figure 27. Confocal images of the cells on the aligned fibrous mat without melatonin at the end of 14 day of tenogenic induction. The cells were immunostained	

against scleraxis (green) and counterstained with DAPI for nucleus (blue).
Magnifications: (a) X20, scale bar: 50 μ m, (b) X40, scale bar: 20 μ m. 58

Figure 28. Confocal images of the cells on the random fibrous mat with melatonin at the end of 14 day of tenogenic induction. The cells were immunostained against scleraxis (green) and counterstained with DAPI for nucleus (blue). Magnifications: (a) X20, scale bar: 50 μ m, (b) X40, scale bar: 20 μ m..... 59

Figure 29. Confocal images of the cells on the random fibrous mat without melatonin at the end of 14 day of tenogenic induction. The cells were immunostained against scleraxis (green) and counterstained with DAPI for nucleus (blue). Magnifications: (a) X20, scale bar: 50 μ m, (b) X40, scale bar: 20 μ m. 60

Figure 30. Confocal images of the cells on the aligned fibrous mat with melatonin at the end of 14 day of tenogenic induction. The cells were immunostained against tenomodulin (green) and counterstained with DAPI for nucleus (blue). Magnifications: (a) X20, scale bar: 50 μ m, (b) X40, scale bar: 20 μ m. 61

Figure 31. Confocal images of the cells on the aligned fibrous mat without melatonin at the end of 14 day of tenogenic induction. The cells were immunostained against tenomodulin (green) and counterstained with DAPI for nucleus (blue). Magnifications: (a) X20, sc scale bar: 50 μ m, (b) X40, scale bar: 20 μ m. 62

Figure 32. Confocal images of the cells on the random fibrous mat melatonin at the end of 14 day of tenogenic induction. The cells were immunostained against tenomodulin (green) and counterstained with DAPI for nucleus (blue). Magnifications: (a) X20, scale bar: 50 μ m, (b) X40, scale bar: 20 μ m. 63

Figure 33. Confocal images of the cells on the random fibrous mat without melatonin at the end of 14 day of tenogenic induction. The cells were immunostained against tenomodulin (green) and counterstained with DAPI for nucleus (blue). Magnifications: (a) X20, scale bar: 50 μ m, (b) X40, scale bar: 20 μ m. 64

LIST OF TABLES

Table 1. Process parameters of electrospinning and their effects on fiber morphology	19
Table 2. Optimization of electrospinning parameters	26
Table 3. The expression of cell surface antigens of DP MSCs (P3).	45



SUMMARY

Tendon injury is an important musculoskeletal problem that causes pain, limited movement, and even immobilization in severe case; therefore, it affects the quality of patient's life. Tendon tissue engineering is a promising approach to restore the function of damaged tendon tissues. Guided tissue engineering is preferred to mimic well-organized tissues like tendon. Stem cells are potential cell sources in tissue engineering and regenerative medicine. The scope of this study was to develop a tissue-engineered tendon substitute composed of aligned electrospun fibrous mat and tenocytes derived from human dental pulp mesenchymal stem cells. The aligned and random fibrous mats were fabricated by electrospinning, and melatonin was integrated into a set of fibrous mats during fabrication considering the ultimate aim which was to enhance regeneration of the tendon tissue. Dental pulp mesenchymal stem cells (DP MSCs) seeded on polymeric scaffolds were induced to differentiate into tenocytes. Cell proliferation and cell orientation on fibrous mats were investigated. To evaluate differentiation, the expression of tenocyte markers, scleraxis and tenomodulin, were investigated by immunocytochemistry. It was observed that DP MSCs were aligned along the axis of fibers on the aligned fibrous mat, while the cells were spread in all direction on random fibrous mat. The cells increased in number on both fibrous mats regardless of surface texture. It was observed that DP MSCs were differentiated to tenocyte-like cells, particularly on aligned fibrous mats. The results indicate that this guided, tissue engineered tendon tissue substitute including DP MSCs could be a potential therapeutic approach for tendon injuries.

Keywords: Tendon, Tissue Engineering, Dental Pulp Mesenchymal Stem Cells, Guided Platform, Electrospun Fibrous Mat

ÖZET

Yönlü Platformlar ve Mezenkimal Kök Hücreler Kullanarak Tendon Doku Mühendisliği Yaklaşımı

Tendon hasarı, ağrıya, sınırlı harekete ve hatta ciddi vakalarda hareketsizliğe neden olan, bu nedenle hastanın yaşam kalitesini etkileyen önemli bir kas-iskelet sistemi problemidir. Tendon doku mühendisliği, hasarlı tendon dokularının işlevini düzeltmek için umut verici yaklaşımlardan biridir. Tendon gibi iyi organize olmuş dokuları taklit etmek için yönlü doku mühendisliği tercih edilir. Kök hücreler doku mühendisliği ve rejeneratif tıpta potansiyel hücre kaynaklarıdır. Bu çalışmanın amacı, elektroğırme ile elde edilen yönlü fiber yapılar ve insan dış pulpası mezenkimal kök hücrelerinden türetilen tenositlerden oluşan tendon doku eşdeğerini doku mühendisliği yöntemiyle geliştirmektir. Yönlü ve düzensiz fiber yapılar, elektroğırme ile üretildi ve nihai hedef olan tendon dokusunun rejenerasyonunu arttırmak için imalat sırasında bir dizi lifli mat içine melatonin entegre edildi. Dış pulpası mezenkimal kök hücreleri (DP MKH) polimerik doku iskelelerine ekildi ve tenositlere farklılaşmaları için uyarıldı. Fiber yapılar üzerinde hücre çoğalması ve hücre yönlenmesi incelendi. Farklılaşmayı değerlendirmek için, tenosit markerleri, skleraksis ve tenomodulin ekspresyonu immünohistokimya ile araştırıldı. DP MKH'lerinin yönlü fiber yapılar üzerinde fiber eksenine boyunca uzandığı, düzensiz fiber yapılar üzerinde ise her yöne yayıldığı görüldü. Yüzey dokusu ne olursa olsun, hücreler fiber yapılar üzerinde sayıca artmıştır. DP MKH'lerin doku iskelelerinde, özellikle yönlü fiber yapılarda, tenosit benzeri hücrelere farklılaştığı gözlemlendi. Elde edilen sonuçlar doku mühendisliği ile geliştirilen DP MKH'leri içeren bu yönlendirilmiş tendon doku eşdeğerinin tendon hasarlarında potansiyel bir tedavi yaklaşımı olabileceğini göstermektedir.

Anahtar Kelimeler: Tendon, Doku Mühendisliği, Dış Pulpası Mezenkimal Kök Hücreleri, Yönlendirilmiş Platformlar, Elektroğırilmiş Fiber Yapı

1. BACKGROUND and AIM OF THE STUDY

Acute and chronic tendon injuries are commonly seen in musculoskeletal clinical problems. Even though the majority of these injuries are nonfatal, they affect daily work performance and reduce the quality of patient's life, and may lead to high cost to the healthcare system. Although the biology of the tendon and the mechanism of tendon repair are well known, researchers and clinicians have not yet found precise treatment strategies. Current tendon treatments, even surgical interventions, have demonstrated limited success, which shows the need for alternative approaches like tissue engineering.

In tissue engineering mimicking extracellular matrix (ECM) and cell organization of the target tissue is very critical to obtain a functional tissue substitute. The organization of tendon extracellular matrix (ECM) molecules at micrometer and nanometer levels has a multi-unit hierarchical structure of collagen fibrils, fascicles, and tendon units. Guided tissue engineering is a promising approach to mimic the well-organized tendon tissue architecture to achieve better and faster integration with the native tissue, and to enhance the healing process. Mesenchymal stem cells are ideal cell sources to be used in regenerative medicine and tissue engineering with their ability to differentiate into various committed mature cells like tenocytes.

The aim of the study was to develop a tissue-engineered tendon substitute using guided platforms as aligned electrospun mats and dental pulp mesenchymal stem cell derived tenocyte-like cells. In addition, melatonin was integrated into scaffolds to increase collagen secretion considering the ultimate which was to enhance regeneration of the tendon tissue. The developed, native tissue-like, oriented tendon substitute could be a promising approach for tendon injuries and could be a patient specific treatment as containing mesenchymal stem cells.

2. INTRODUCTION

2.1 Tendon Tissue

The anatomic structure of the tendon is important due to being attachment region between muscle and bone (Figure 1a). Tendon tissue transmits the muscle forces to the bone, and thus allows joint motion and maintains movement of body. A healthy tendon color is brilliant white, and it has a fibro-elastic structure. Tendon tissue is resistant to mechanical loads, especially tensile forces. Since it is bound to bones, tendon shape may significantly change from wide and flat tendon to cylindrical and ribbon-shaped tendon. Muscles producing resistive forces, like the quadriceps and triceps brachii muscles possess short and broad tendons, whereas muscles carrying out delicate movements, like the finger flexors possess long and thin tendons. Each muscle has two tendon regions as proximal and distal parts. Muscle to tendon interface is called as myotendinous junction (MTJ), while bone to tendon interface is called as osteotendinous junction (OTJ). The tendon tissue is surrounded by fibrous sheath, reflection pulleys, synovial sheath, paratenon and the tendon bursae (1).

Tendon tissue is composed of a dense regular connective tissue which is characterized by ordered and densely packed arrays of collagen fibers and cells which are oriented along the fibers (Figure 1b). The main component of the tendon tissue is high amount of Type I collagen fibers which are arranged in a cross-linked triple-helix structure. In ECM of tendon, these collagen fibers aligned in the direction of the long axis of the tendon are found in parallel bundles, called tendon fascicles, and a small amount of elastin fibers are found in proteoglycan-water matrix. Besides collagen and elastin, tendon ECM contains proteoglycans, glycosaminoglycans, and also inorganic components like calcium. The progenitor cells, tenoblasts and the elongated fibroblast type cells, tenocytes, are the cellular components of tendon tissue. A thin layer of loose connective tissue, known as paratenon, surrounds many tendons. Main function of paratenon is to allow free movement of the tendon against

the surrounding tissue by sliding. Under the paratenon, the entire tendon is surrounded by a fine connective tissue sheath called epitenon. The epitenon contains a relatively dense network of longitudinal, oblique collagen fibrils. Epitenon fibrils fuse with the superficially located tendon fibrils and with the endotenon on the inner surface. The endotenon is composed of a thin reticular connective tissue binds tendon fascicles (1, 2, 3).

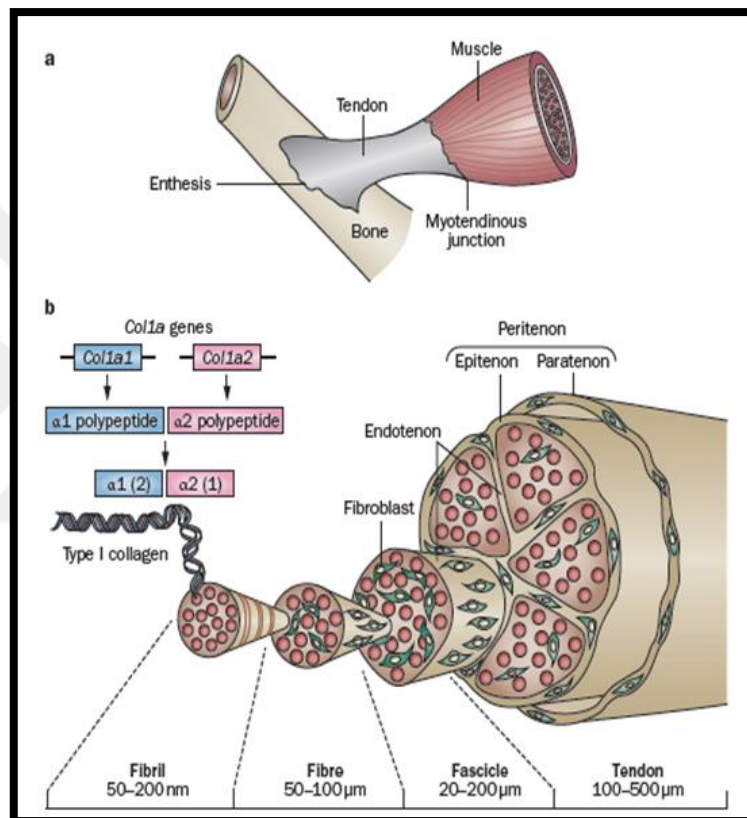


Figure 1. (a) Anatomical structure and (b) organization of tendon tissue

Reference: Geoffroy Nourissat, Francis Berenbaum and Delphine Duprez. Tendon injury: from biology to tendon repair. *Nature Reviews, Rheumatology*, 2015; 223–233.

2.2 Tendon Damages

Tendon pathologies vary from chronic injury to acute injury depending on the level of tendon damage. Chronic tendon injury or tendinopathy displays clinical symptoms including pain, focal tendon tenderness, decreased in strength, and restricted movement in affected tendons. Tendinopathy could be identified with some histopathological indications such as disorganization of collagen fibrils, accumulation of proteoglycans and glycosaminoglycans, and formation of noncollagenous ECM. In addition, hypercellularity and neovascularization are seen in tendinopathy. The other tendon injury type, acute tendon injury is a result of partial or complete tear (rupture). Partial or complete tear impairs the tendon continuity and leads to loss of movement (4). A limited natural healing process is occurred after tendon rupture, even though this is one of the least efficient healing in musculoskeletal system.

Many intrinsic and extrinsic factors promote chronic and acute tendon injuries (5). The prevalent intrinsic risk factors are sex, age, and some diseases such as type 2 diabetes mellitus and obesity. The main recognized extrinsic factor of tendon injuries is abnormal loading on tendon tissues which can be done during physiological exercise, sport, and hard-working conditions. Most tendinopathies are associated with many factors. Tendons at certain regions, like shoulder, elbow, knee and ankle, are exposed to high mechanical forces, therefore tendons in that regions have high degeneration rate and more affected by injury resulting in rotator cuff tear, supraspinatus tear, patellar tear and Achilles tendon tear (6).

2.3 Treatment Methods of Tendon Injuries

Treatments for chronic tendon injuries (tendinopathy) or acute tendon injuries mainly aim to reduce pain. Depending on damage type, location and size, there are different treatment methods from well-known techniques to up to date approaches. These methods can be surgical procedures or nonsurgical treatments of damaged tendon (4,7).

The challenge in surgical repair is to provide the best tendon stability without shortening tendon. Generally, tendon is repaired with core sutures and running circumferential epitendinous suture. Many different core suture techniques are given in Figure 2. The success of surgical tendon treatments is affected by many factors such as tension applied during repair, number of runs, properties of suture materials (8).

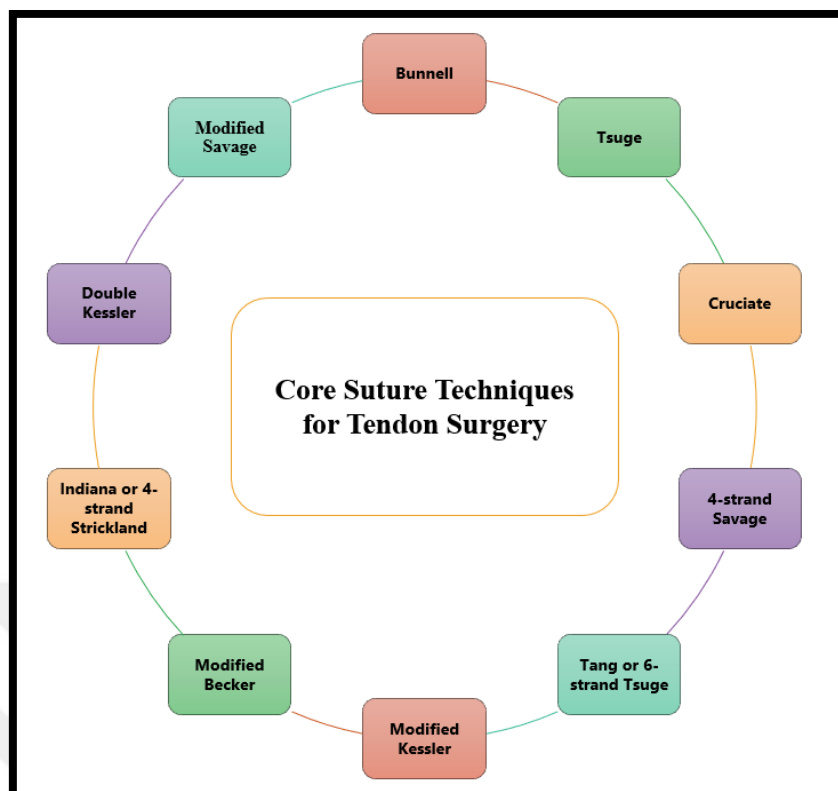


Figure 2. Different core suture techniques for tendon surgery

Reference: Gloria R. Sue, James Chang. Tendon Repair. James Chang. Global Reconstructive Surgery. 2020.

Nonsurgical methods are medication with topical or systemic anti-inflammatory drugs, exercise-based rehabilitation, particularly eccentric exercise therapy, using autologous growth factors as platelet-rich-plasma (PRP) to promote tissue healing, extracorporeal shock-wave therapy particularly in calcified tendinitis of the shoulder. There are also alternative approaches for tendon treatment such as therapeutic ultrasonography or low-level laser therapy, stem cell-based therapy, biomaterials and tissue engineering applications (4,9).

2.4 Tendon Tissue Engineering

Tissue engineering is an interdisciplinary field that applies the principles of engineering and life sciences. The tissue engineering aims to develop biological substitutes to restore the damaged tissues or organs that are incapable of functioning properly. The challenge in tissue engineering is to mimic the target tissue in terms of its architecture, composition, organization and mechanical properties. Tissue engineering is composed of three factors as cell source, cell carrier known as scaffold, and bioactive agents (Figure 3) (10).

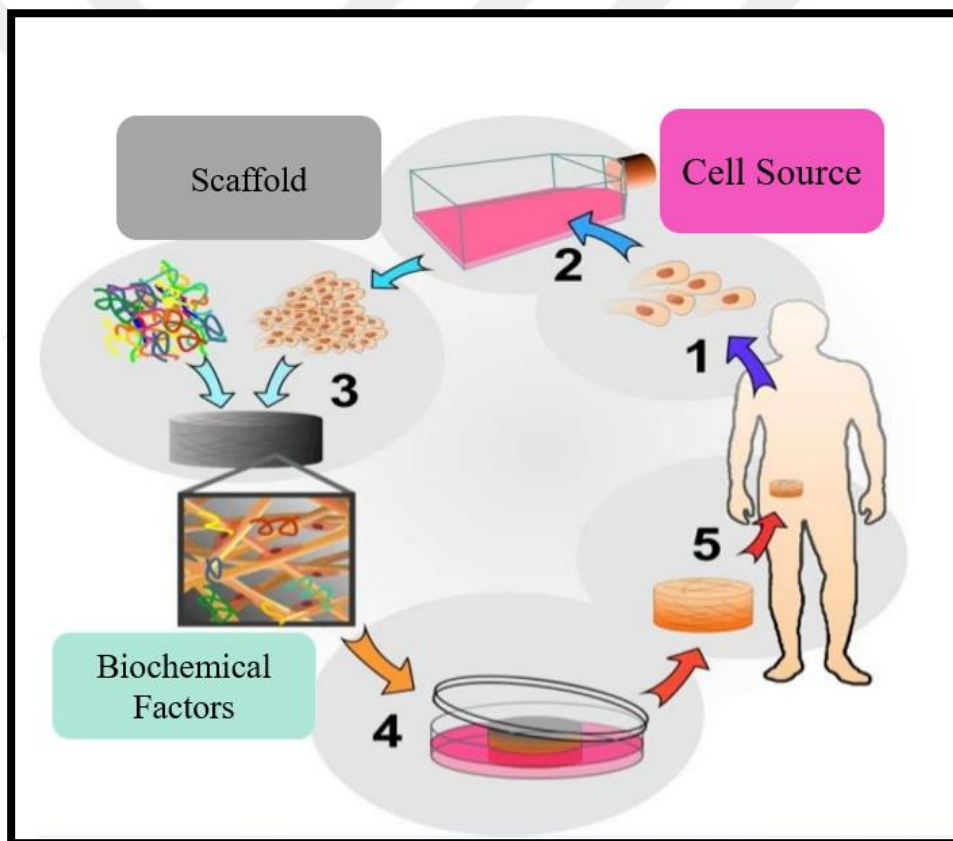


Figure 3. Principles of tissue engineering

Reference: https://www.lehigh.edu/~inbios21/PDF/Fall2015/Chow_10302015.pdf

In particular tissues like nerve, skeletal muscle, cardiac muscle and tendon, the cells are well organized and oriented by the aid of extracellular matrix. Guided tissue engineering is utilized to mimic these well-organized tissues in order to achieve better and faster integration with the native tissue, and to enhance the healing process. In tendon tissue engineering topography guided platforms are integrated into scaffold design to mimic organization of tendon ECM and to align cells like in native tissue. The combination of biochemical and physical factors in a dose and time-dependent manner play a key role for obtaining successfully engineered tendon (11).

2.4.1 Cell Sources

Stem cells have taken a significant role in tissue engineering and regenerative medicine (12). The emerging applications prefer these unspecialised cells due to their favorable properties as their self-renewal capacity and differentiation into various cell types. According to their stage of stemness, they are categorized as totipotent, pluripotent and multipotent (Figure 4). Totipotent stem cells has the highest self-renewal and differentiation capacity. Pluripotent stem cells can differentiate into any cell type of the body derived from three germ layers, endoderm, mesoderm and ectoderm. However, multipotent stem cells can differentiate into cell types of a specific tissue. Stem cells are also classified according to their origin as embryonic stem cells (ESCs), mesenchymal stem cells, hematopoietic stem cells, neural stem cells, skin stem cells, etc. (13).

Embryonic stem cells (ESCs) that are pluripotent stem cells derived from the inner cell mass (ICM) of early stage embryos (12). Embryonic stem cells are promising cell sources for stem cell and tissue engineering studies due to their high self-renewal and differentiation capacity. They can differentiate into any cell type of the body derived from three germ layers, endoderm, mesoderm, and ectoderm (13). However, there are serious ethical concerns with ESCs and their risk of teratoma formation restricts their use, especially in clinical applications.

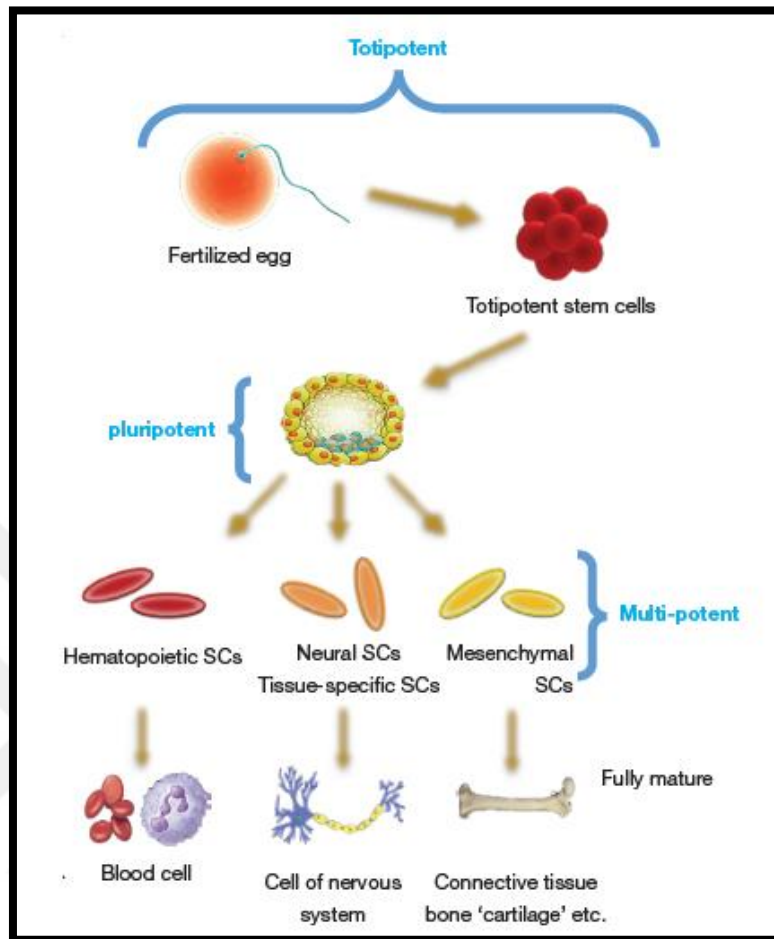


Figure 4. Classification of stem cells

Reference: (<http://sci.amegroups.com/article/viewFile/27241/html/168687>)

2.4.1.1 Mesenchymal Stem Cells

Mesenchymal stem cells (MSCs) have self-renewable capacity providing increase in cell number, and they have multilineage differentiation potential, particularly at early passages (Figure 5) (14). Under *in vitro* conditions, MSCs preserve their morphology in undifferentiated state up to a certain sub-culture. Mesenchymal stem cells have a natural tendency to differentiate into mesoderm derived osteocytes, adipocytes, chondrocytes (15). However, they can also differentiate into other mesodermal derived tissue cells like muscle, ligament, and tendon. In addition, the researchers showed that under specific induction conditions MSCs can also differentiate into the cells that are derived from ectoderm and endoderm such as neurons, hepatocytes, etc. MSCs express cell surface antigens like cluster of differentiation CD44, CD73, CD90, CD105, while they have negative expression of hematopoietic markers, CD34, CD45 and human leukocyte antigen HLA-DR (14,15).

Human mesenchymal stem cells were firstly isolated from bone marrow (13). Later studies showed that human MSCs have been isolated from various tissues such as adipose tissue (16), umbilical cord (17), placenta (18), amniotic membrane (19), amniotic fluid (20), dental pulp (21, 22).

Human MSCs have been widely preferred to be used in tissue engineering and regenerative medicine applications due to being clinically safe, having advantageous properties regarding immune response, being easily obtainable from various adult tissues (14). MSCs also show paracrine effect, they can regulate some processes like proliferation, angiogenesis, immunomodulation, and tissue regeneration (23). MSCs have been utilized for the treatment of various tissues like nervous tissue, myocardium, liver, cornea, trachea, skin, etc. The use of MSCs have been widely seen especially in tissue engineering of musculoskeletal system tissues like bone, cartilage, muscle, and tendon (24).

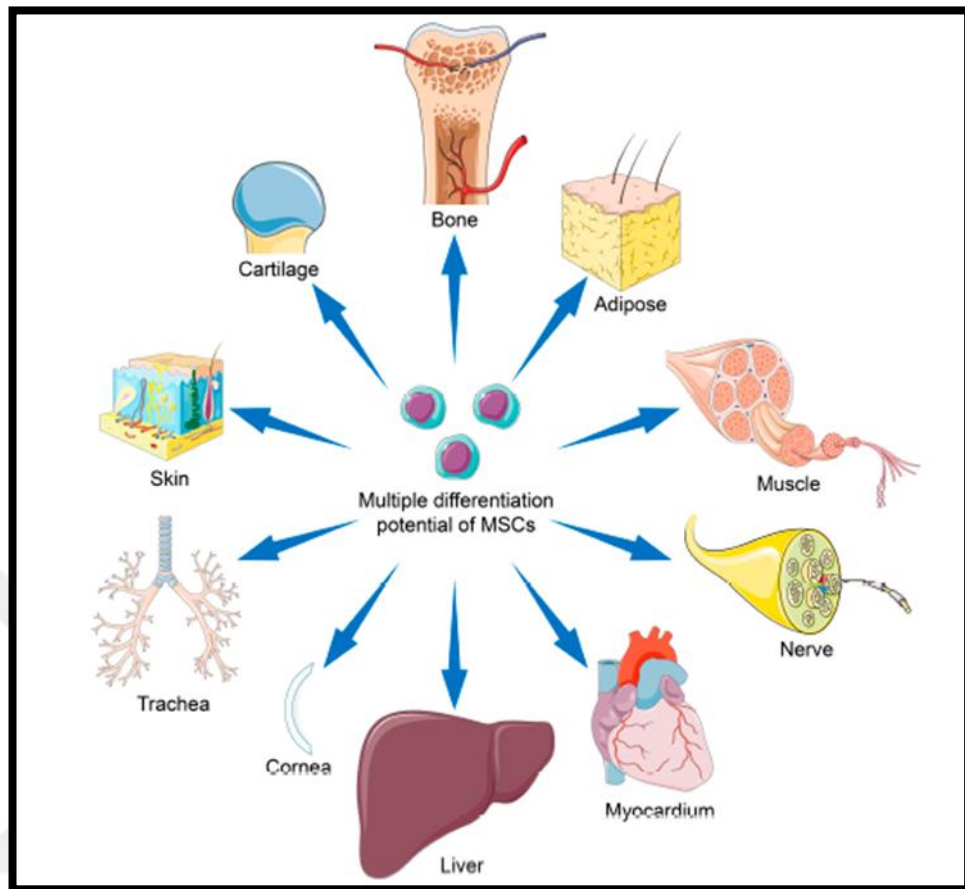


Figure 5. Multiple differentiation potential of mesenchymal stem cells for repair of various tissues.

Reference: Yu Han, Xuezhou Li, Yanbo Zhang , Yuping Han, Fei Chang and Jianxun Ding. Mesenchymal Stem Cells for Regenerative Medicine. Cells. 2019

2.4.2 Scaffold for Tendon Tissue Engineering

Scaffold, also called a cell carrier, is a supporting structure to provide cell attachment and cell growth. The scaffold mimics the natural ECM of tissues; therefore, it should provide an appropriate physical and functional milieu for cells like ECM. The scaffold should be biocompatible, sterilizable to avoid any contamination. The scaffold should possess a porous architecture for cell penetration and transportation of nutrients and oxygen. In addition, the production process of the scaffold should be reproducible and economical. The scaffold materials should be chosen according to the properties of target tissue (25). In addition, the architecture of the scaffold should resemble 3D ECM structure of the target tissue to perform specific tissue functions. The cells seeded on the scaffold could undergo proliferation, migration, and even differentiation to form a target tissue. In the body there are well-organized tissues like nervous tissue, myocardium, skeletal muscle and tendon tissues. The scaffolds designed for these well-organized tissues should preferably involve guided platforms.

By developing tissue engineering strategies novel scaffold designs are offered for the treatment of tendon disorders. The scaffold used in tendon tissue engineering should withstand mechanical loading considering tendon function. (26, 27, 28). Various biological and synthetic scaffolds have been utilized in tendon tissue engineering studies (29, 30). The topography guided platforms such as micro-nano patterns/channels or aligned fibrous meshes could be utilized in scaffolds for tendon tissue engineering.

2.4.2.1 Natural Scaffolds

Natural scaffolds are derived from natural tissues and these can be either decellularized extracellular matrix (ECM) from allografts and xenografts or can be made up of natural polymers isolated from tissue samples (31). Natural scaffolds obtained from tissues of human cadaver, porcine, bovine, and equine have been utilized in tendon tissue engineering studies (32). Decellularization process involves the following cascade steps. These steps include general cleaning, removal of lipids or fat deposits, disruption of cells including its DNA materials, crosslinking, and then sterilization of scaffold. The scaffolds fabricated with natural polymers, are predominantly composed of natural collagen fibers, particularly type I collagen, for tendon tissue engineering. Besides collagen, gelatin and elastin have been widely used in the scaffold construction for tendon tissue (25). Natural scaffolds with their biologically active chemistry promote cell proliferation and tissue growth (32). Biological scaffolds display high biocompatibility, but they have some limitations such as low mechanical stability and immunogenicity. Therefore, in the scaffold design biological polymers can be used with synthetic polymers to eliminate the limitations of both biological and synthetic polymers.

2.4.2.2 Synthetic Scaffolds

Synthetic polymers can be biodegradable like poly(lactic acid) (PLA), poly(glycolic acid) (PGA), and poly(lactic-co-glycolic acid) (PLGA), etc., or can be nondegradable like poly(ethylene) (PE), poly(ethylene terephthalate) (PET), and poly(tetrafluoro ethylene) (PTFE). In tissue engineering studies biodegradable polymers are preferred since they are disappeared after regeneration of damaged tissue. PLA, one of the most widely used synthetic polymers in tissue engineering, is biodegradable, biocompatible, non-toxic, and non-immunogenic. Optically active L- and D-lactides form poly(L-lactide)

(PLLA) and poly(D-lactide) (PDLA), respectively. The choice and distribution of stereoisomers within the polymer chains differ the mechanical properties, and biodegradation characteristics of lactic acid polymers (33). The higher crystallinity feature of the polymer results in stronger and stiffer scaffolds (34). The other commonly used biodegradable synthetic polymer in tissue engineering is poly(lactic-co-glycolide) (PLGA) which is the copolymer of poly(lactic acid) (PLA) and poly(glycolic acid) (PGA) (34, 35, 36). PLGA can be prepared at different ratios of monomers, lactic (LA) and glycolic acid (GA). It can be dissolved in various organic solvents such as chloroform, tetrahydrofuran, acetone or ethylacetate (34, 37). Degradation of PLGA is occurred by hydrolysis of its ester linkages in aqueous environments through bulk or heterogeneous erosion. The biological safety and tuneable degradation properties makes PLGA a potential polymer used for scaffolds in tissue engineering (38).

2.4.3 Fabrication of Guided Platforms via Electrospinning

Advances in engineering technologies results in emerging different strategies in fabrication of scaffolds. Various forms of scaffolds are produced by different fabrication methods such as freeze-drying, solvent casting, gas foaming, particulate leaching, rapid prototyping, and fiber-production techniques. Various fiber-production techniques are used to obtain fibrous mesh scaffolds (Figure 5) (39). Particularly the aligned fibrous meshes are preferred in guided, tendon tissue engineering considering the anisotropic organization of the tendon tissue.

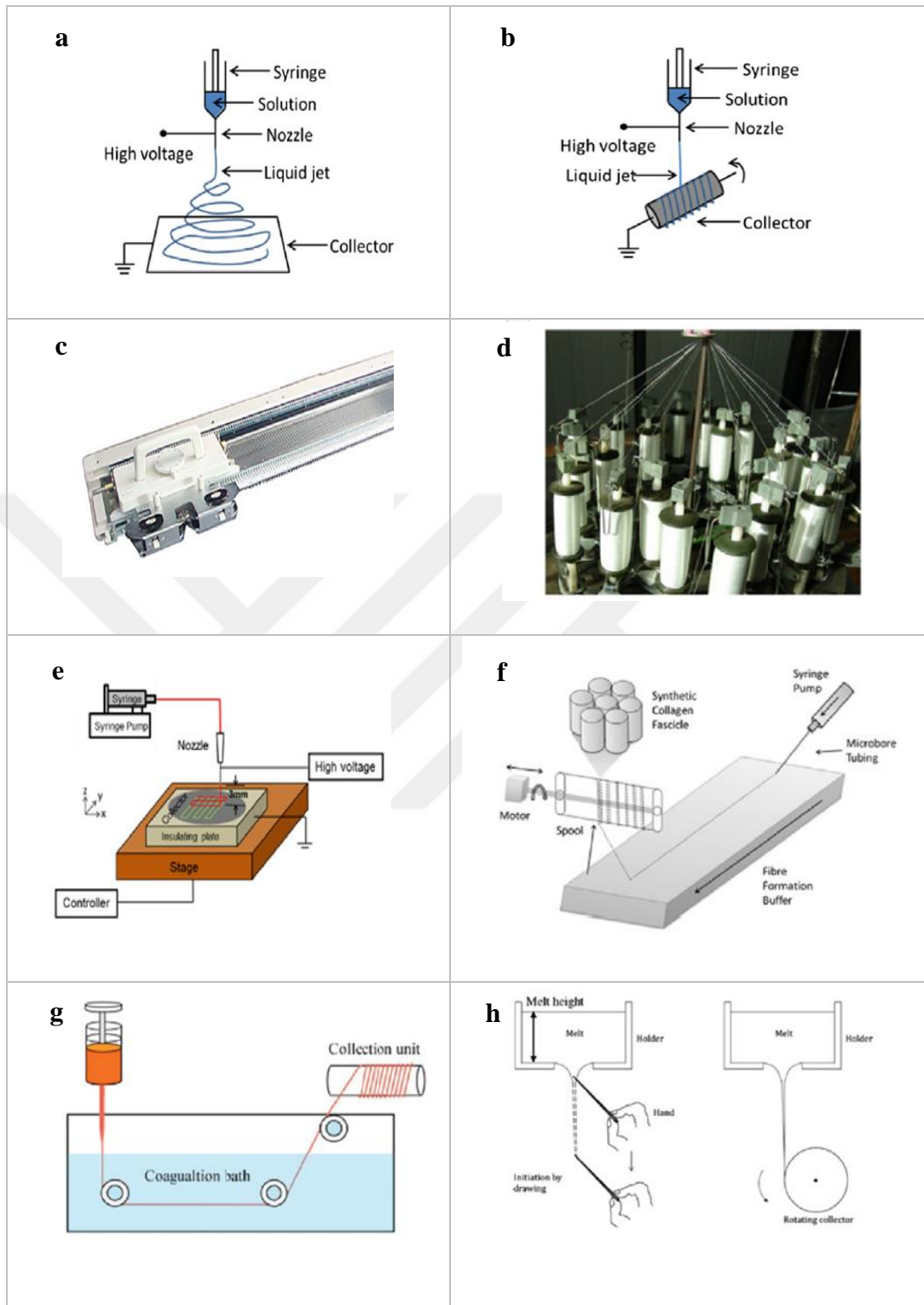


Figure 6. Schematic illustrations of fiber-production techniques used for scaffolds in tendon tissue engineering. (a) electrospinning of random fibers, (b) electrospinning of aligned fibers, (c) knitting, (d) braiding, (e) E-jetting (f) extrusion, (g) wet spinning and (h) microfiber melt drawing.

(Han, Yang Wu and Yi. 3D functional scaffolds for tendon tissue engineering. Functional 3D Tissue Engineering Scaffolds. 2018; Chapter 15.)

One of the fiber-production techniques is electrospinning. The system includes three major components: i) spinneret, ii) metal collector and iii) power supply. The spinneret is a metal nozzle attached to a syringe containing the polymer solution to be electrospun. The polymer solution is pushed at a certain flow rate with syringe pump. The power supply applies high voltage to form electrical field between a small diameter needle and a metal collector. Upon potential application, a pendent droplet of polymers solution at the needle tip is charged, and polymer jet is forced to eject and deposited on the collector as in fiber form (40). The electrospinning process parameters such as viscosity and conductivity of polymer solution, flow rate, applied potential, the distance between collector and nozzle tip, etc. affect the morphology, size and organization of electrospun fibers (Table 1) (41). By controlling fiber diameter and fiber orientation, electrospinning serves many advantages in scaffold fabrication. Electrospinning is a cost-effective and versatile technique to produce polymeric fibers, of which diameter range microns to nanometers. In addition, electrospun fibrous scaffolds are favourable in tissue engineering with their ultra-fine fibers, porosity, high surface area to volume ratio (25). Electrospinning has been widely utilized in manufacturing 3D scaffolds for tendon tissue engineering.

Tissues contain nanoscale structures and these structures assist tissue-specific functions. Tissues are classified into four types according to function; the protective tissue as skin, the electro-active tissues as nervous system, skeletal muscle, heart, the shear stress-sensitive tissue blood vessel, and the mechano-sensitive tissues as bone, ligament/tendon. Mechano-sensitive tissues like tendon are exposed to mechanical forces, walking or exercise. Tendon, a nanostructured tissue, has multilevel, hierarchical, and staggered organization, and this is critical for its function (42). The anisotropic organization of tendon provides needed mechanical strength, and sufficient dynamic action by inter-fiber sliding (43,44).

Table 1. Process parameters of electrospinning and their effects on fiber morphology (Reference 41)

Process parameter	Effect on fiber morphology
<i>Viscosity / concentration</i>	<ul style="list-style-type: none"> ✓ Low concentrations/viscosities yielded defects in the form of beads and junctions; the defects are reduced by increasing concentration/viscosity ✓ Fiber diameters increased with increasing concentration/viscosity
<i>Conductivity / solution charge density</i>	<ul style="list-style-type: none"> ✓ Increasing the conductivity aided in the production of uniform bead-free fibers ✓ Higher conductivities yielded smaller fibers in general (exceptions were PAA and polyamide-6)
<i>Surface tension</i>	<ul style="list-style-type: none"> ✓ No conclusive link established between surface tension and fiber morphology
<i>Polymer molecular weight</i>	<ul style="list-style-type: none"> ✓ Increasing molecular weight of polymer reduced the number of beads and droplets
<i>Dipole moment and dielectric constant</i>	<ul style="list-style-type: none"> ✓ Successful spinning is occurred in solvents with a high dielectric constant
<i>Flow rate</i>	<ul style="list-style-type: none"> ✓ Lower flow rates yielded fibers with smaller diameters ✓ High flow rates produced fibers that were not dry upon reaching the collector
<i>Field strength / voltage</i>	<ul style="list-style-type: none"> ✓ At too high voltage, beading was observed ✓ Correlation between voltage and fiber diameter was ambiguous
<i>Distance between tip and collector</i>	<ul style="list-style-type: none"> ✓ A minimum distance was required to obtain dried fibers ✓ At distances either too close or too far, beading was observed
<i>Needle tip design</i>	<ul style="list-style-type: none"> ✓ Using a coaxial, 2-capillary spinneret, hollow fibers were produced ✓ Multiple needle tips were employed to increase throughput
<i>Collector composition and geometry</i>	<ul style="list-style-type: none"> ✓ Smoother fibers are obtained with metal collectors; more porous fiber structure was obtained using porous collectors ✓ Aligned fibers were obtained using a conductive frame, rotating drum, or a wheel-like bobbin collector ✓ Yarns and braided fibers were also obtained
<i>Ambient parameters</i>	<ul style="list-style-type: none"> ✓ Increased temperature caused a decrease in solution viscosity, resulting in smaller fibers ✓ Increasing humidity resulted in the appearance of circular pores on the fibers

2.4.4 Bioactive Agents

Bioactive agents such as growth factors, hormones, proteins, peptides, etc. can be integrated into scaffolds to enhance cell survival, growth, differentiation, migration and tissue regeneration in order to facilitate healing process. Melatonin (N-acetyl-5-methoxytryptamine) is a hormone produced by the pineal gland under the control of nervous and endocrine systems. The studies on melatonin mechanism showed that its function depends not only on circadian rhythms but also on seasonal changes (45). Melatonin displays a known anti-inflammatory and pro-chondrogenic effect on cells. In addition, melatonin possesses various functions like reducing inflammation and apoptosis in the treatment of Osteoarthritis (OA). Melatonin has been widely used in regenerative medicine applications. A study on tendon-to-bone healing models showed that melatonin-loaded polycaprolactone (PCL) membranes might promote chondrogenic differentiation of human bone marrow derived mesenchymal stem cells (hBMSCs) (46). As a result, melatonin could be a potential bioactive agent to be integrated into scaffold in tissue engineering applications.

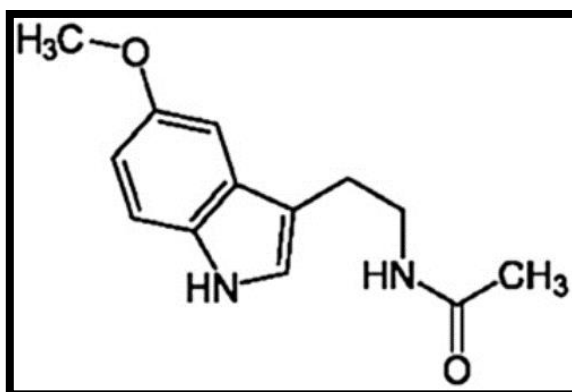


Figure 7. Chemical structure of melatonin

Reference: Ambriz-Tututi M, Rocha-González HI, Cruz SL, Granados-Soto V. Melatonin: a hormone that modulates pain. (15-16):489-498. Life Sciences, 2009.

3. MATERIALS AND METHODS

3.1 Materials

Poly(L-lactide-co-D,L-lactide) (P(L-D,L)LA) (70:30, 1 500 000 g/mol) and poly(lactide-co-glycolide) (PLGA) (50:50, 153 000 g/mol) were purchased from Purac Company. Fibronectin was purchased from Gibco. Chloroform and dichloromethane were obtained from Sigma Aldrich. α -MEM, DMEM low glucose and DMEM high glucose, Fetal Bovine Serum (FBS), Penicillin/Streptomycin (Pen/Strep) and PBS solutions were purchased from Gibco. Trypsin-EDTA, FITC-phalloidin and 4',6-diamidino-2-phenylindole dihydrochloride (DAPI) were obtained from Sigma. MTS kit was obtained from Promega. All antibodies for flow cytometry analysis were purchased from BD Biosciences. GDF-7/BMP-12 was obtained from Novus. Scleraxis and tenomodulin primary antibodies and secondary antibody Alexa fluor 488 were purchased from Thermo Fisher.

3.2 Methods

The experiments performed in this study were summarized in Figure 8.

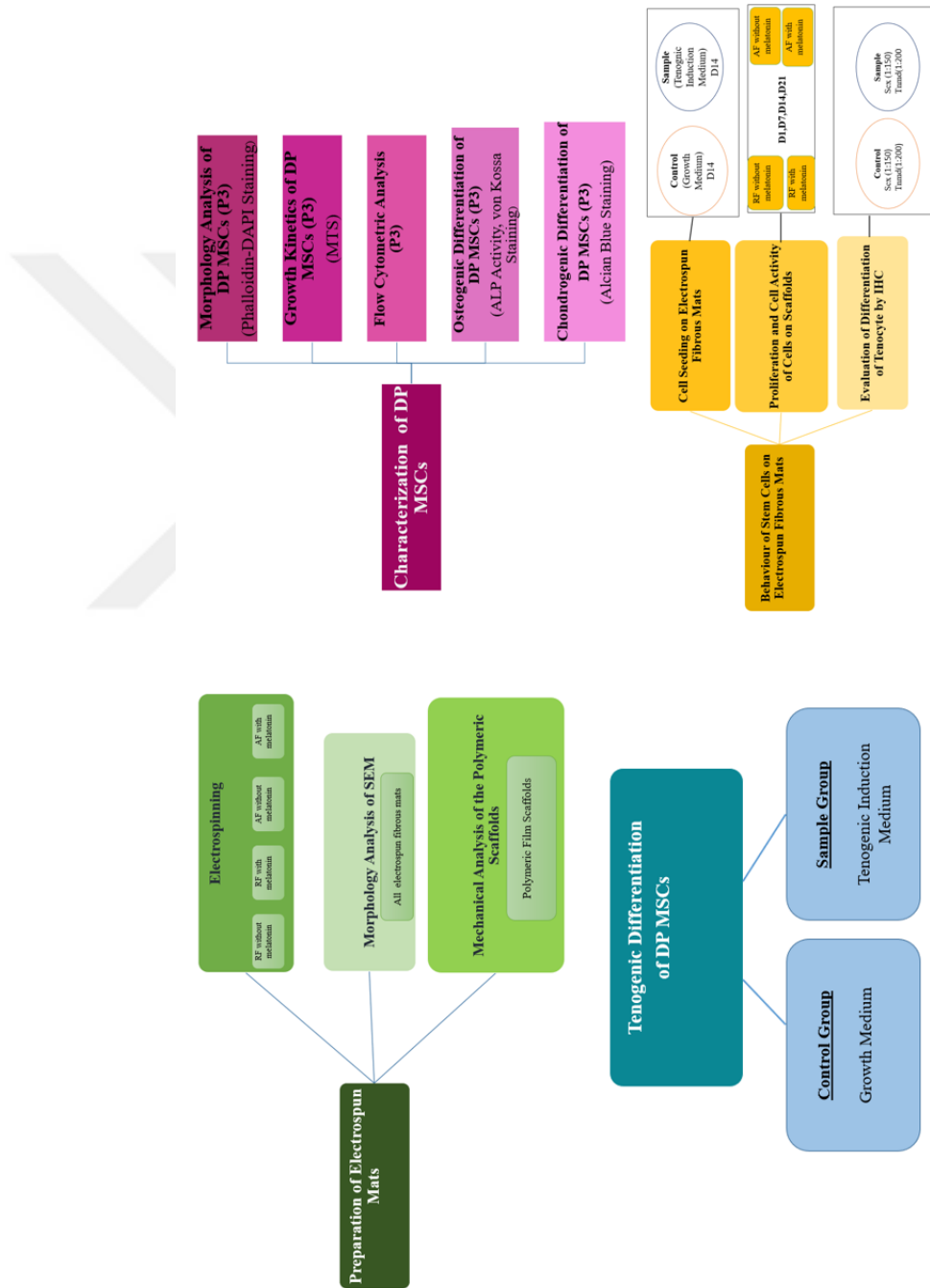


Figure 8. Experimental design of the study

3.2.1 Preparation of Scaffolds

3.2.1.1 Fabrication of Electrospun Fibrous Mats

Electrospinning was used to obtain micro/nano fibers. The electrospinning system was comprised of a high voltage supply (Inovenso Ne100 Modified Model), a 10 mL syringe capped with a 23 Ga needle, syringe pump, and a metal collector. The random fibers were produced using metal plate collector. On the other hand, the aligned fibers were obtained using the collector that had two metal rods, and the fibers were collected between these rods as a parallel aligned fibrous mat. The electrospinning process was performed in a closed hood to minimize environmental influences such as temperature and relative humidity.

A polymer blend solution was filled into a syringe, and then the syringe was placed onto a syringe pump (Figure 9). The positive electrode of high voltage source was connected to the metallic needle of the syringe to charge the polymer solution, while the collector end was grounded. When a high voltage was applied, the repulsive electrostatic forces overcame the surface tension of the polymer solution. A Taylor cone, a conical shaped droplet of solution, was formed at the tip of needle, and it was expelled and deposited on the collector as a micro/nano fiber (Figure 9). Fiber thinning and solvent evaporation were occurred during this process.

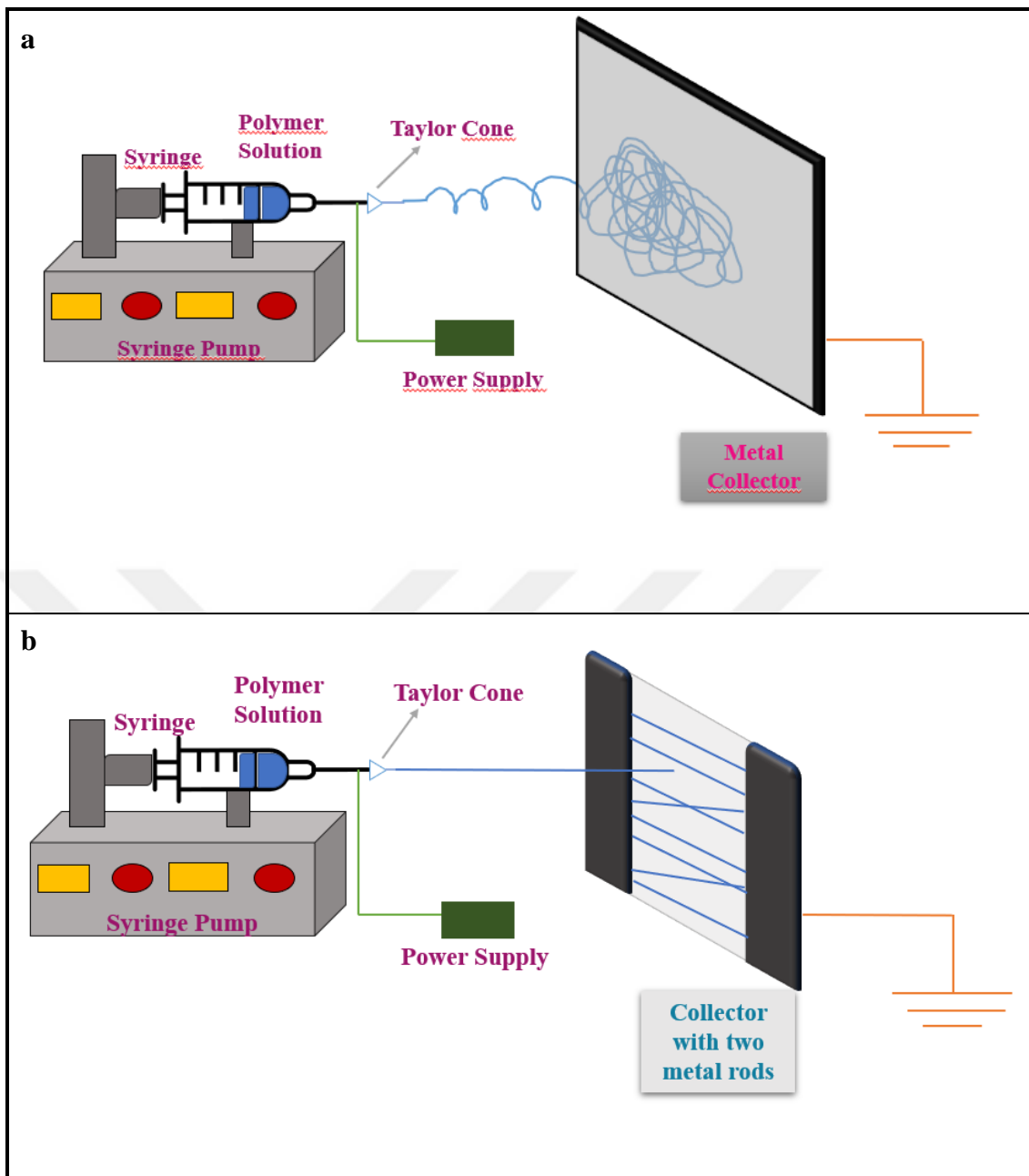


Figure 9. Schematic illustration of electrospinning system to fabricate (a) random fibrous mat and (b) aligned fibrous mat.

The polymer blend solution of P(L-D,L)LA and PLGA (1:1, w:w) was prepared in chloroform (Chl) with a concentration of 5% (w/v). Dimethylformamide was added into polymer solution (polymer solution:DMF, 8:2) to increase the conductivity of polymer for electrospinning process. The final electrospun polymer solution was 3% (w/v) of P(L-D,L)LA-PLGA. A set of electrospun fibers was prepared by integration of melatonin. For that purpose, 50 ng/mL melatonin was added into polymer solution for the group of electrospun fiber with melatonin.

Various parameters were optimized to obtain uniform, bead-free, non-fused, aligned fibers (Table 2). According to optimization results, in the further studies the polymer solution (3%, w/v) was electrospun according to the following process conditions; the distance between syringe needle and collector (25 cm), the flow rate (20 μ L/min) and the applied potential (10 kV).

Table 2. Optimization of electrospinning parameters

Polymer Concentration (%)	Potential (kV)	Distance (cm)	Flow Rate ($\mu\text{l}/\text{min}$)	Syringe Diameter (mm)	Observations
3	11	25	12	15	The fibers were not aligned Bead formation was seen
3	14	25	12	15	No bead formation was observed Thick fibers were formed
3	12	25	10	15	Bead formation was seen
3	12	25	11	15	Bead formation was seen
3	12	25	15	15	Bead formation was seen
3	10	25	8	16.25	The ejection of polymer solution was discontinuous Thin fibers were formed
3	10	25	12	16.25	The ejection of polymer solution was discontinuous Bead formation was seen
3	10	25	20	25	The fibers were uniform and aligned Bead formation was not observed, bead-free fibers were obtained

3.2.1.2 Morphology Analysis of the Scaffolds by Scanning Electron Microscopy

Electrospun fibrous mats were coated with 20 nm gold (Au) and examined under high vacuum with Scanning Electron Microscope (SEM, Thermo Scientific Quattro ESEM) in Electron Microscopy Laboratory at Acıbadem Mehmet Ali Aydınlar University. The fiber diameter distribution and fiber deviation angles were determined by Fibra Quant Software using SEM images of the scaffolds.

3.2.1.3 Mechanical Analysis of the Polymeric Scaffolds

Mechanical tests of polymeric scaffolds were carried out at the Center of Excellence in Biomaterials and Tissue Engineering, Middle East Technical University (BIOMATEN, METU). Polymeric films (P(L-D,L)LA-PLGA (0.25 mm in thickness, 1cm in width and 5 cm in length) were attached to holders of the mechanical tester (CellScale Mechanical Testing ,Univert). The samples were tested under a 1 mm/sec test speed. The stress-strain curve was obtained, and the Young's Modulus of the sample was determined from the slope of straight line in elastic region of the stress-strain curve.

3.2.2 *In Vitro* Studies

3.2.2.1 Isolation and Culture of Human Dental Pulp Mesenchymal Stem Cells

Human dental pulp mesenchymal stem cells (DP MSCs) used in this study were isolated by explant culture during another study of Deniz Yücel. Human dental pulp MSCs were used with the approval of ethical committee (Acibadem Mehmet Ali Aydınlar University, Istanbul, ATADEK given in Appendix 2). Briefly, deciduous teeth of 6 to 12 years healthy children were supplied in PBS containing penicillin/streptomycin (Pen/Strep, 100 unit/mL-100 µg/mL). Dental pulp tissues were cut into small pieces, transferred into tissue culture plates and cultivated in 1 mL of growth medium containing Alpha MEM (α MEM) supplemented with 10 % Fetal Bovine Serum (FBS), and 100U/mL-100µg/ml Pen/Strep in a CO₂ incubator (5% CO₂) at 37°C. After 12 hours of incubation, 1 mL growth medium was added into plates and the culture was continued by changing medium every 3 days. When DP MSCs reached 70-80% confluency, cells were detached with 0.05% Trypsin-EDTA, and subcultured (passaged) by seeding into new tissue culture flasks. Cells were frozen in 10% DMSO and stored in vapor of liquid nitrogen. Human DP MSCs at passage 3 were used in the further studies.

3.2.2.2 Characterization of Dental Pulp MSCs

3.2.2.2.1 Morphology Analysis of DP MSCs

In order to investigate the morphology and cytoskeletal organization of human DP MSCs, the cells were stained with FITC conjugated phalloidin for their actin filaments and counterstained with DAPI for their nucleus. DP MSCs at P3 were seeded with a density of 10⁴ cells/well into 24 well plates in the

growth medium and cultured. The cells were fixed on day 3 with 4% paraformaldehyde (PFA in PBS) for 30 min at room temperature, and then washed two times with PBS. The cells were permeabilized by incubation in 0.1% Triton X-100 (in PBS) for 10 min at room temperature, and then washed with PBS three times. To prevent nonspecific binding, the cells were incubated in blocking solution of 1% bovine serum albumin (BSA) for 30 min at 37°C. After blocking, the cells were incubated in FITC-Phalloidin (1:100 in 0.1% BSA) for 1 h at 37°C. Following washing with PBS, the cells were counterstained with DAPI (1:5000 in PBS) for 10 min. After washing with PBS, the cells were examined under laser scanning confocal microscope (Zeiss, LSM 700).

3.2.2.2.2 Growth Kinetics of Dental Pulp MSCs

DP MSCs at passage 3 were seeded into 24 well plates at a density of 10^4 cells/well in the growth medium and cultured in CO₂ incubator at 37°C. The samples were studied in triplicate (n=3). The cell number was determined by the CellTiter 96® Aqueous One Solution Cell Proliferation Assay (MTS Assay) at certain time points of culture. MTS assay is based on the reduction of tetrazolium compound found in MTS / PES solution by metabolically active cells into a coloured formazan product which gives an absorbance at 490 nm.

At the time points 24, 48, 96, 144, 168 and 240 h of culture, the growth medium of cells in 24 well plate was discarded, and then 0.5 mL MTS/PES working solution (10% MTS/PES solution prepared with DMEM Low Glucose, 10% FBS and 100 unit/mL-100 µg/mL Pen/Strep) was placed onto the cells. The cells were incubated in MTS/PES solution for 2 h at 37°C in CO₂ incubator. After incubation, 0.2 mL solution was transferred into 96 well plates to determine the absorbance of the coloured product of MTS assay at 490 nm with

Elisa Plate Reader (Thermo Scientific 5250030-Varioskan Flash Multi Mode Reader). The obtained absorbance values were converted to cell number using the calibration curve (Appendix 1).

3.2.2.2.3 Flow Cytometry Analysis

Specific surface antigens of the isolated DP MSCs at passage 3 were analysed with flow cytometer (BD Sciences, FACS Verse). Cell surface markers, hematopoietic lineage markers like CD34, CD45, MSC markers like CD105, CD73, CD44 and CD90, and immunogenic antigens like HLA-ABC, HLA-DR were investigated. DP MSCs were detached by trypsinization and counted. The cell pellet of 5×10^5 cells was resuspended in 1% BSA (in PBS). Fluorochrome conjugated antibodies against the indicated surface antigens were added into cell suspension. The samples were incubated with antibodies for 1 hour at 4°C. After incubation, the samples were centrifuged at 2200 rpm for 5 min, and then fixed with 1% PFA (in PBS). The cells were analysed with flow cytometer to determine the percentage of cells that expressed the indicated cell surface antigens. An isotype control was taken into consideration in each experiment to remove non-specific binding signal.

3.2.2.2.4 Osteogenic Differentiation of Dental Pulp MSCs

Considering MSCs have natural tendency to osteogenic differentiation, the isolated dental pulp cells were differentiated into osteoblasts to show that the isolated cells were MSCs. For that purpose, DP MSCs at P3 were seeded at a density of 10^4 cells/well into 24 well plates and cultured in the growth medium. After one day of culture in the growth medium, osteogenic induction medium composed of DMEM low glucose supplemented with 10 % FBS, 100 U/mL-100

$\mu\text{g/ml}$ Pen/Strep, 100 nM dexamethasone, 50 $\mu\text{g/mL}$ ascorbate-2-phosphate and 10 μM β -glycerophosphate was applied onto cells. The cells were cultured in this induction medium for 14 and 21 days at 37°C in CO₂ incubator, and the induction medium was refreshed twice a week. The cells cultured in the growth medium were used as control. The osteogenic differentiation was assessed after 14 and 21 days of culture by alkaline phosphatase (ALP) activity and von Kossa staining.

For ALP activity analysis on 14 and 21 days of osteogenic differentiation, the cells were lysed with 0.1 % Triton X-100 (in 0.1 M, pH 7.6 Tris Buffer) and the lysed samples were centrifuged at 5000 rpm at 4°C for 10 min. After centrifugation, the lysate in supernatant part was mixed with 0.1 % Triton X-100, and then the substrate p-nitrophenyl phosphate and the reaction buffer were added. The product of the reaction given below, p-nitrophenol was measured at 405 nm within two minutes intervals for 16 minutes by spectrophotometer (Thermo Scientific 5250030-Varioskan Flash Multi Mode Reader). The solution containing all the reagents except the cell lysate was used as a blank.

The deposition of CaP by cells upon osteogenic differentiation was determined by von Kossa staining. At 14 and 21 days of differentiation, cells were washed with PBS two times, and they were fixed with 4% PFA for 30 min at room temperature. Following washing with PBS and distilled water, the fixed samples were incubated with 1% aqueous silver nitrate solution under ultraviolet light (UV) for 1 hour. After rinsing with distilled water three times, the cells were incubated in 5% sodium thiosulfate for 5 min at room temperature. Following washing with distilled water, the samples were examined under light microscope (Zeiss, Primovert Inverted Microscope).

3.2.2.2.5 Chondrogenic Differentiation of Dental Pulp MSCs

The isolated cells were differentiated into chondroblasts to show that they were MSCs. Dental pulp MSCs at passage 3 were seeded at a density of 5×10^3 cells/well into 24 well plates in the growth medium. After one day of culture, chondrogenic induction medium composed of DMEM Low Glucose supplemented with 10 % FBS, 100 U/mL-100 μ g/ml Pen/Strep, 100 nM dexamethasone, 40 μ g/mL proline, 1 μ M ascorbate-2-phosphate, 1 % sodium pyruvate and 1 % Insulin-Transferrin-Selenium (ITS) was applied for 14 and 21 days in CO₂ incubator at 37°C by changing induction medium twice a week. The control groups were cultured in the growth medium. Chondrogenic differentiation was assessed by Alcian blue staining after 14 and 21 days of culture. At the end of 14 and 21 days, the samples were washed with PBS and the cells were fixed 4% PFA for 1 hour at room temperature. Following washing with PBS, the samples were stained with 1 % Alcian Blue (pH 2.5 in 3 % acetic acid) for 30 min at room temperature. After staining, the samples were washed under running tap water for 2 min. The samples were examined under light microscope (Zeiss, Primovert Inverted Microscope).

3.2.2.3 Tenogenic Differentiation of Dental Pulp MSCs

DP MSCs at P3 with a density of 5×10^4 cells/well were seeded on fibronectin (50 μ g/mL) coated surfaces and cultured in the growth medium overnight. After one day, the growth medium was replaced with tenogenic induction medium containing DMEM Low Glucose supplemented with 1% FBS, 100 U/mL-100 μ g/mL Pen/Strep and 100 ng/mL GDF7/BMP12. The cells were treated with induction medium for 14 days by refreshing twice a week.

After differentiation for 14 days, the cells were washed with PBS and the cells were fixed 4% PFA for 30 min at room temperature. Following washing with PBS,

the samples were immunostained for the expression of tenogenic markers, tenomodulin and scleraxis. The cells were incubated in 100 mM glycine for 15 min to saturate reactive PFA groups. After washing with PBS, the cells were permeabilized by Triton X-100 (0.1% in PBS, PBST) treatment for 10 min at room temperature. After washing, the cells were incubated in 1% BSA (in PBS) at 37°C for 1 h to block nonspecific binding of antibodies. The cells were incubated with primary antibodies, anti- scleraxis (1:150 in 0.1% BSA) and anti-tenomodulin (1:200 in 0.1% BSA) at 4°C overnight onto shaker. After incubation with primary antibodies, the cells were washed with PBS and then the fluorescence labeled secondary antibody Alexa Fluor 488 (1:100 in PBS) was applied for 1 h at 37°C, and then washed with PBST, and subsequently with PBS. The cells were counterstained with DAPI (1:5000 in PBS) for 10 min and washed with PBS. The cells were examined with laser scanning confocal microscope (Zeiss, LSM 700).

3.2.2.4 Behaviour of Stem Cells on Electrospun Fibrous Mats

3.2.2.4.1 Cell Seeding on Electrospun Fibrous Mats

The electrospun fibrous mats were sterilized with UV treatment for 1 h. Before cell seeding, the scaffolds were coated with fibronectin (50µg/mL) for 1 h. Dental pulp MSCs at P3 were seeded onto fibronectin coated electrospun mats at a density of 2×10^4 cells / sample ($1 \times 1 \text{ cm}^2$) for cell organization and proliferation and 4×10^4 cells / sample ($1 \times 1 \text{ cm}^2$) for differentiation analysis, respectively. For proliferation and cell organization analysis the cells were cultured with growth medium (α MEM supplemented with 10 % FBS and 100 U /mL-100 µg/ml Pen/Strep). For differentiation studies, the cells were cultured in tenogenic induction medium (DMEM Low Glucose supplemented with 1% FBS, 100 U/mL-100 µg/ml Pen/Strep and 100 ng/mL GDF7/BMP12) for 14 days by refreshing twice a week. The cells cultured with growth medium was used as undifferentiated control.

3.2.2.4.2 DP MSC Organization on the Scaffolds

Dental Pulp MSCs' organization and their alignment on the electrospun fibrous mats (without melatonin) were investigated by Phalloidin and DAPI staining for actin organization and nucleus, respectively. DP MSCs at P3 were seeded with a density of 7.5×10^5 cells/well into 24 well plates and cultured in the growth medium. On 7th day of culture, the cells were fixed with 4% PFA (in PBS) for 30 min at room temperature, and then washed with PBS. The cells were permeabilized with 0.1% Triton X-100 (in PBS) for 10 min at room temperature, and then washed with PBS. To prevent nonspecific binding, the cells were incubated in blocking solution of 1% BSA for 30 min at 37°C. After blocking, the cells were incubated in FITC- Phalloidin (1:100 in 0.1% BSA) for 1 h at 37°C. Following washing with PBS, the cells were counterstained with DAPI (1:5000 in PBS) for 10 min. After washing with PBS, the cells were examined under laser scanning confocal microscope (Zeiss, LSM 700).

3.2.2.4.3 Proliferation and Cell Activity of DP MSCs on the Scaffolds

To assess proliferation and cell activity of the cells, the number of DP MSCs on the electrospun mats with and without melatonin were determined by Cell Titer 96* AQueous One Solution Cell Proliferation Assay (MTS Assay).

The cells at a density of 2×10^4 cells/sample were seeded onto fibronectin coated electrospun mats with and without melatonin and onto TCPS. The cells were cultured with growth medium in CO₂ incubator. The samples were studied in triplicate (n=3). At the end of 1, 7, 14 and 21 days of culture, the scaffolds were transferred into new 24 well plate, and then 0.5 mL MTS/PES working solution (10% MTS/PES solution prepared with DMEM Low Glucose, 10% FBS and 100 unit/mL-100 µg/mL Pen/Strep) was placed on the cells. The cells

were incubated in MTS/PES solution for 2 h at 37°C in CO₂ incubator. After incubation, 0.2 mL solution was transferred into 96 well plates to determine the absorbance of the coloured product of MTS assay at 490 nm with Elisa Plate Reader (Thermo Scientific 5250030-Varioskan Flash Multi Mode Reader). The obtained absorbance values were converted to cell number using the calibration curve (Appendix 1).

3.2.2.4.4 Evaluation of Tenogenic Differentiation of DP MSCs on The Scaffolds By Immunocytochemistry

DP MSCs were seeded onto electrospun mats with and without melatonin, and tenogenic induction protocol was conducted as the details given in Section 3.2.2.4.2. After 14 days of tenogenic induction, the cells were fixed with 4% PFA for 30 min at room temperature and then washed with PBS. The cells were incubated in 100 mM glycine for 15 min to saturate reactive PFA groups. After washing with PBS, the cells were permeabilized by Triton X-100 (0.1% in PBS, PBST) treatment for 10 min at room temperature. After washing, the cells were incubated in 1% BSA (in PBS) at 37°C for 1 h to block nonspecific binding of antibodies. The samples were immunostained for the expression of tenogenic markers, tenomodulin and scleraxis. The cells were incubated with primary antibodies, anti- scleraxis (1:150 in 0.1% BSA) and anti-tenomodulin (1:200 in 0.1% BSA) at 4°C overnight onto shaker. After washing with PBS, the samples were incubated with secondary antibody, Alexa Fluor 488 (1:100 in PBS) for 1 h at 37°C. After washing with PBST and PBS, the cells were counterstained with DAPI (1:5000 in PBS) for 10 min, and washed with PBS. The cells were examined with laser scanning confocal microscope (Zeiss, LSM 700).

3. RESULTS

4.1 Characterization of Electrospun Mats

4.1.1 Morphology and Dimension Analysis of the Electrospun Fibrous Mats

Morphology and topography of the electrospun fibrous mats were examined by SEM. The polymer blend solutions of P(L-D,L)LA-PLGA (3%, w/v; 1:1, w:w, in Chl:DMF, 8:2) were prepared either including 50 ng/mL melatonin or not. The polymer solutions were electrospun under optimized process conditions as a constant applied potential 10 kV, with flow rate 20 $\mu\text{L}/\text{min}$, a distance of 25 cm. Electrospun fibers with and without melatonin were collected between two metal rods as aligned fibrous mats, while random fibrous mats were collected on smooth metal plate.

SEM results showed that uniform and bead-free fibers were obtained without any fusion in both random and aligned electrospun mats (Figure 10 and 11). The fibers were unidirectionally, well-oriented in the aligned fibrous mats (Figure 10). It was observed that the presence of melatonin did not affect the morphology and topography of both aligned and random fibers. It was determined that the fiber diameter in random fibrous mat was in the ranges of 200-700 nm (Figure 12). It was observed that the fiber diameter in aligned fibrous mat ranged between 300-700 nm, and most of the fibers were 300-400 nm and 500-700 nm in diameter (Figure 13).

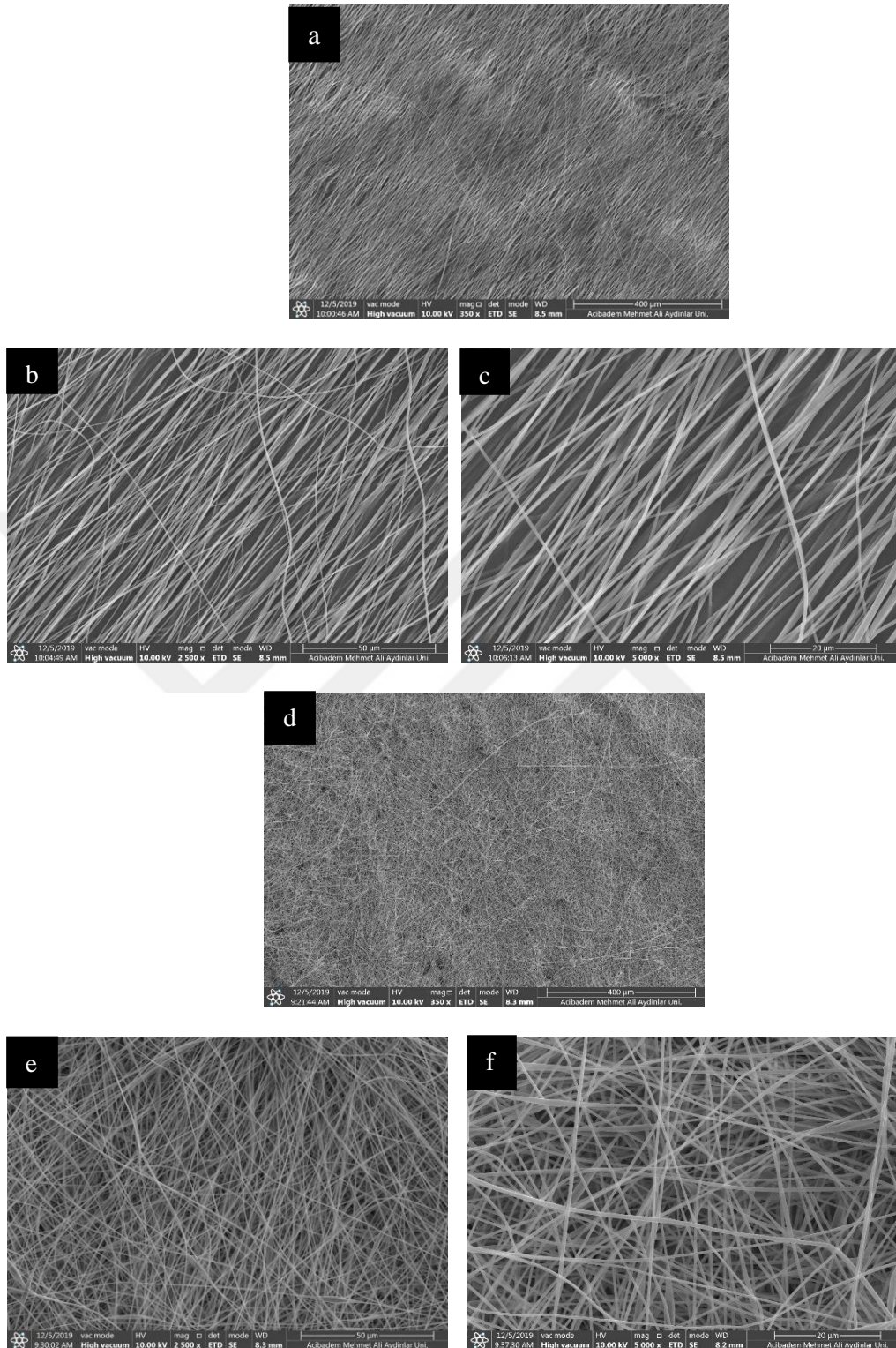


Figure 10. SEM images of P(L-D,L)LA-PLGA electrospun fibers in the absence of melatonin. (a,b,c) Aligned fibrous mat and (d,e,f) random fibrous mat. Magnifications: (a,d) 350X, scale bar: 400µm , (b, e) 2500X, scale bar: 50µm, (c, f) 5000X, scale bar: 20µm.

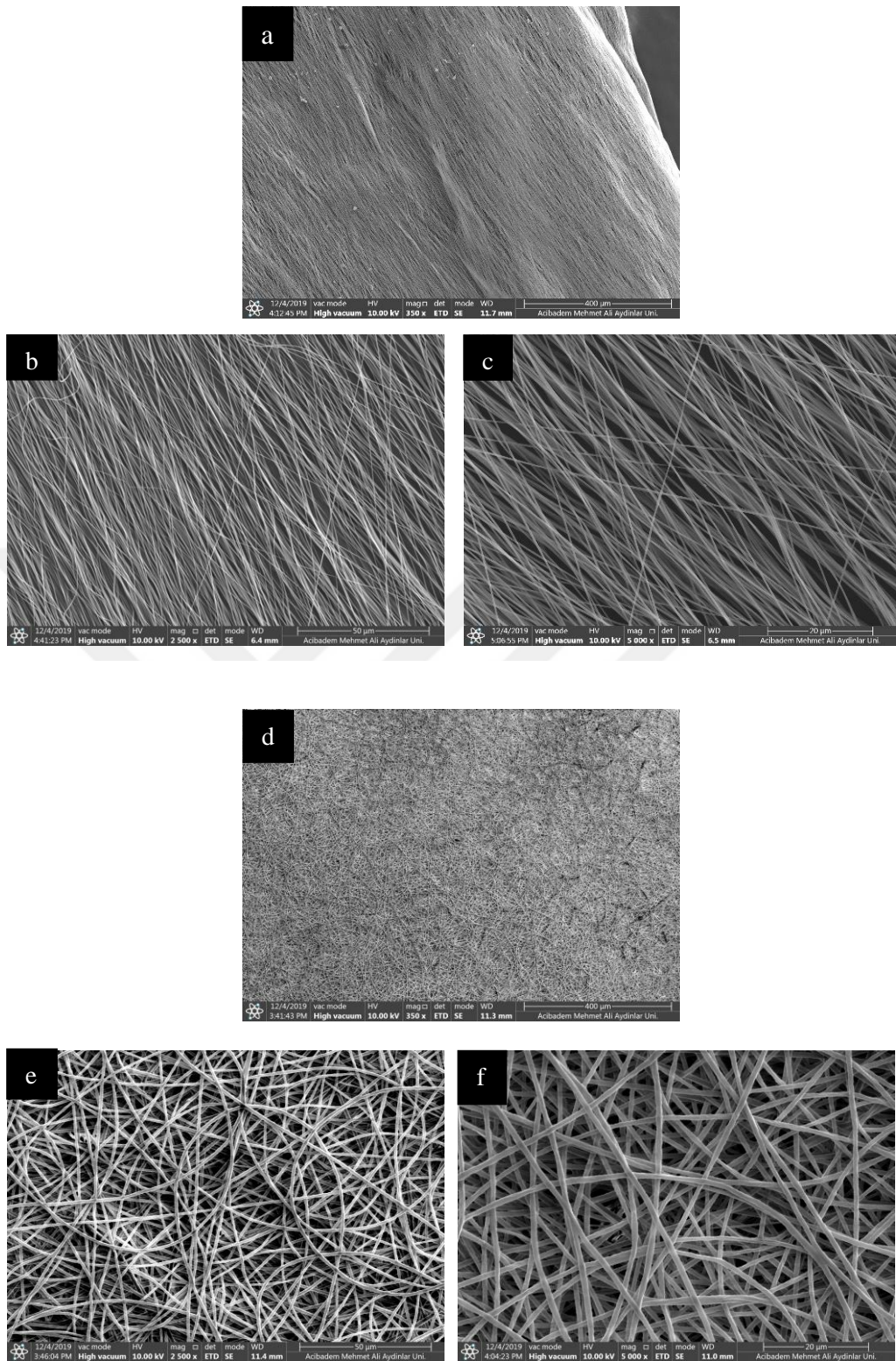


Figure 11. SEM images of P(L-D,L)LA-PLGA electrospun fibers with melatonin group. (a,b,c) Aligned fibrous mat and (d,e,f) random fibrous mat. Magnifications: (a,d) 350X, scale bar: 400µm, (b,e) 2500X, scale bar: 50µm, (c,f) 5000X, scale bar: 20µm

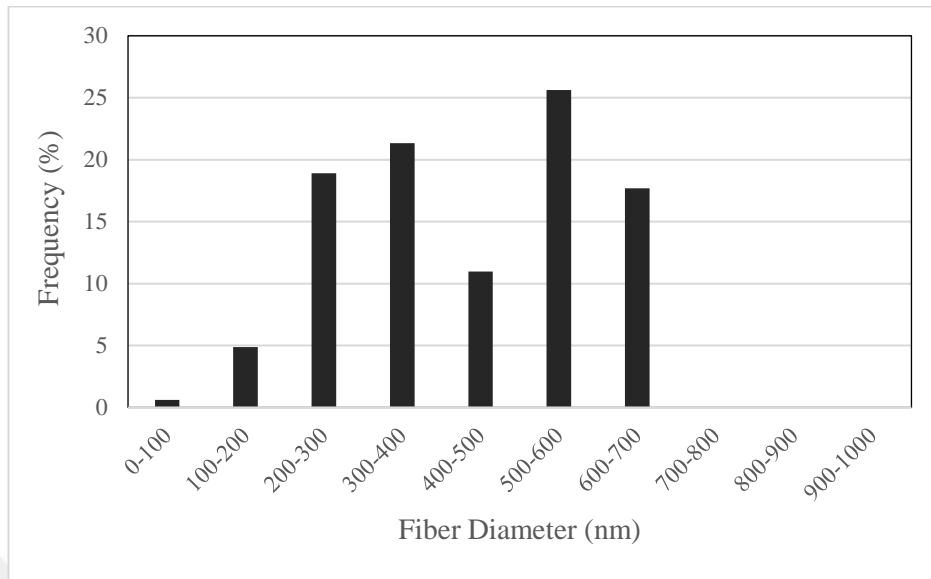


Figure 12. The distribution of fiber diameter of the random fibrous mat

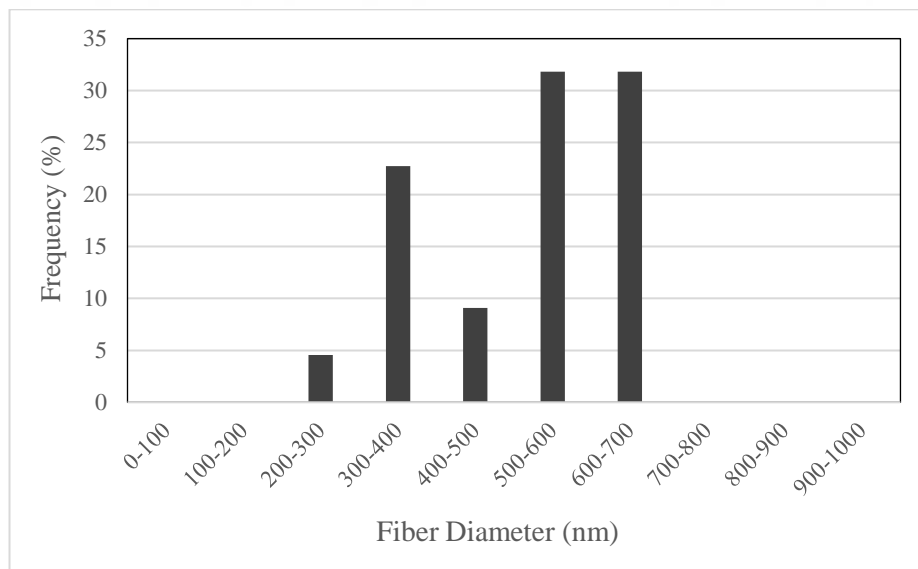


Figure 13. The distribution of fiber diameter of the aligned fibrous mat

4.1.2 Mechanical Analysis of the Polymeric Scaffolds

Mechanical properties of the scaffolds were investigated by stretch-tension test. The representative stress-strain curve obtained by tensile test was given in Figure 14. It was determined that the Young's modulus (E) and yield strength of P(L-D,L)LA-PLGA films were 159.03 ± 24.38 MPa and 4.383 ± 1.117 MPa, respectively.

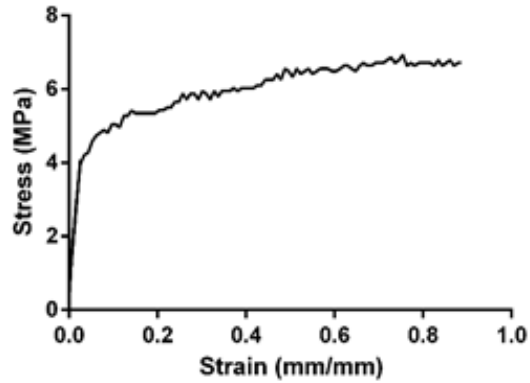


Figure 14. Representative stress-strain curve of tensile test of the polymeric films

4.2 *In Vitro* Studies

4.2.1 Culture and Characterization of Human Dental Pulp MSCs

4.2.1.1 Evaluation of DP MSCs morphology

Morphology of the isolated DP MSCs were examined under light microscope. It was observed that DP MSCs in undifferentiated state exhibited spindle-shaped fibroblast-like morphology (Figure 15). DP MSCs were stained with Phalloidin and DAPI for the cytoskeleton and nucleus, respectively. The results showed that the isolated dental pulp MSCs had flat, spindle shape with well- organized actin filaments and had well-defined spherical nuclei (Figure 16).

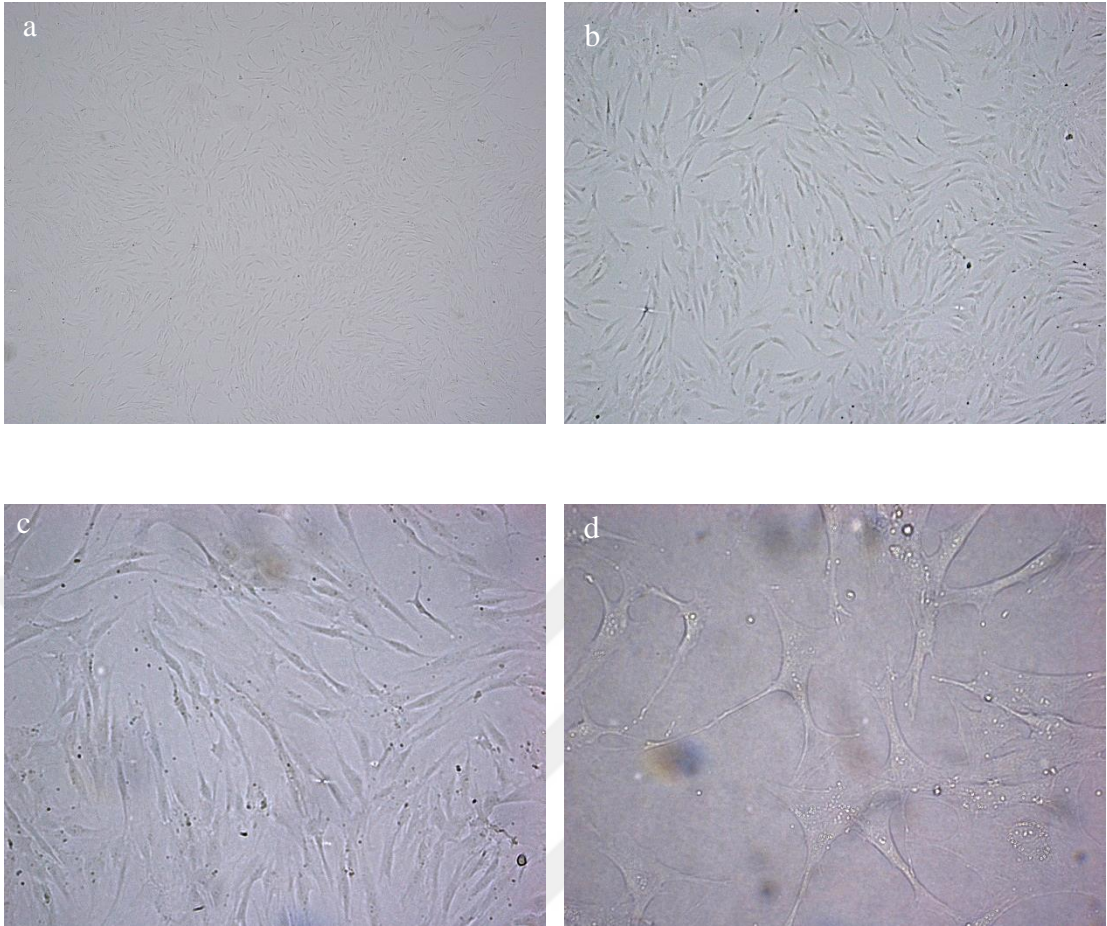


Figure 15. Light microscope images of human DP MSCs (P3). Magnifications: (a) 4X, (b) 10X, (c) 20X, , (d) 40X

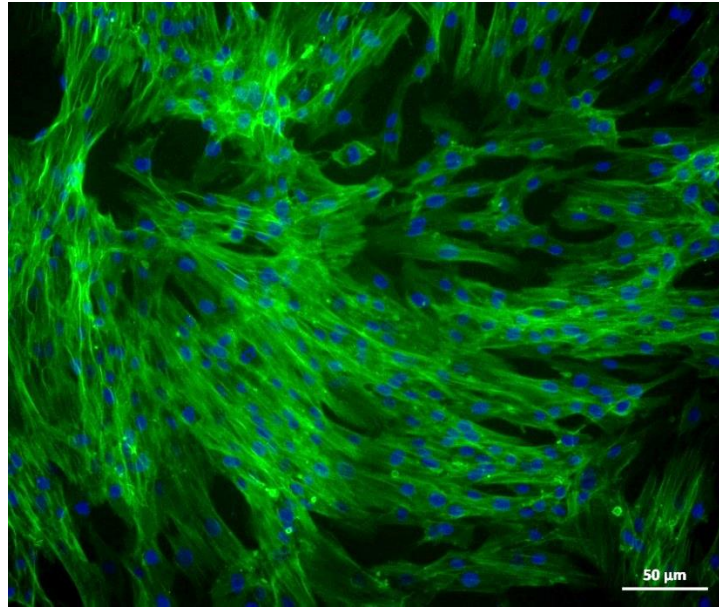


Figure 16. Confocal microscope image of DP MSCs (P3) which were stained with Phalloidin-DAPI for actin filaments (green) and nucleus (blue), respectively. Magnification: 20X, scale bar: 50 μm .

4.2.1.2 Growth Kinetics of Dental Pulp MSCs

The growth kinetics of DP MSCs were shown by plotting the cell number (log number of cells) against time (h). The number of cells was determined by MTS assay using calibration curve of DP MSCs (Appendix 1). It was observed that the cell number was increased exponentially by time, particularly within 50-150 h (Figure 17). The growth increase in number of DP MSCs reached plateau around 240 h of culture. The doubling time of the DP MSC population was calculated as 15 ± 0.3 h from the exponential phase of the growth curve (Figure 17).

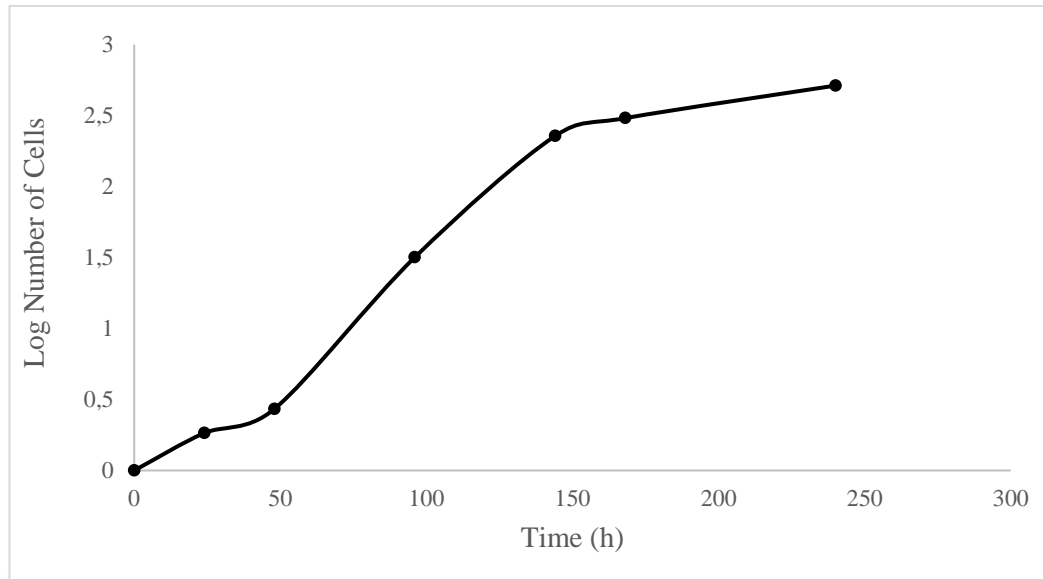


Figure 17. Growth kinetics of human DP MSCs (doubling time: 15 ± 0.3 h)

4.2.1.3 Flow Cytometry Analysis

The expressions of specific cell surface antigens of human DP MSCs at passage 3 were analysed by flow cytometer. The expression of surface antigens of DP MSCs are given in Table 3 considering isotype controls. It was observed that isolated DP MSCs had a positive expression (above 95%) of MSC markers CD105, CD90, CD44 and CD73 and also positive expression of HLA-ABC. However, DP MSCs had very low, almost no, expression (below 1%) of hematopoietic markers CD34 and CD45, and also negative expression for HLA-DR.

Table 3. The expression of cell surface antigens of DP MSCs (P3).

Surface Antigen	DP MSCs %*
CD105	95.47 ± 3.31
CD73	99.33± 0.66
CD90	99.44± 0.74
CD44	99.38± 0.76
HLA -ABC	98.59± 1.15
CD45	0.63± 0.25
HLA-DR	0.27± 0.22
CD34	0.03± 0.02

*Percentage of cells that expressed these surface antigens (Absolute positive values were calculated considering the intersection of isotype control and sample graphs)

4.2.1.4 Osteogenic Differentiation of Dental Pulp MSCs

The osteogenic differentiation of DP MSCs was determined by ALP enzyme activity and CaP deposition. Alkaline phosphatase (ALP) is an enzyme secreted by osteoblasts in the early stages of mineralization. It is responsible for the removal of phosphate from many phosphates carrying calcium salts. DP MSCs induced to differentiate into osteoblasts were investigated for their ALP enzyme activity which shows osteogenic differentiation. ALP activity was defined as nmole substrate converted to product per min, and specific ALP activity was determined by calculating ALP activity per μg of total protein. It was observed that specific ALP activity of DP MSCs treated with osteogenic induction was higher compared to undifferentiated DP MSCs for both 14 days and 21 days (Figure 18). In addition, there was a slight increase in specific ALP activity on 21st day of osteogenic induction compared to 14th day result.

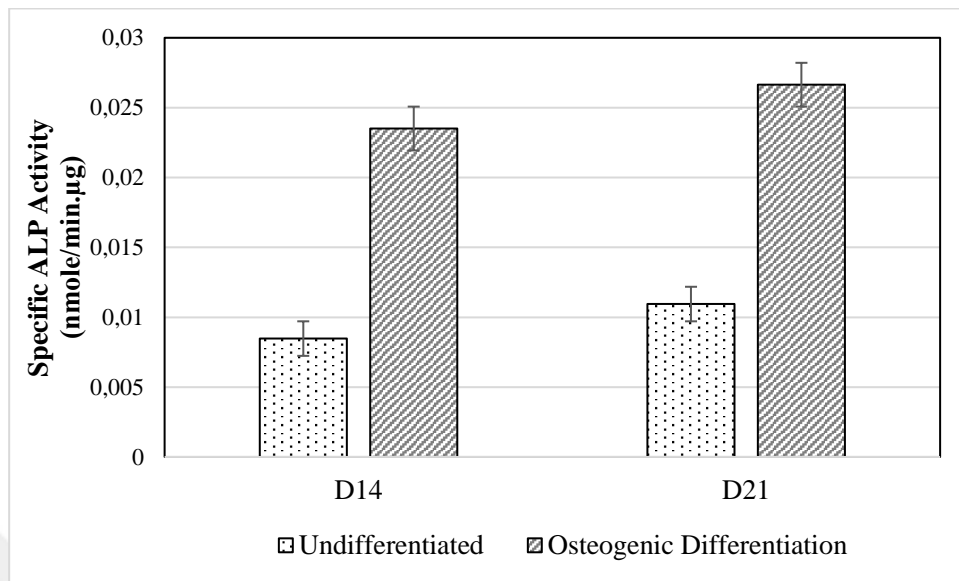


Figure 18. Specific ALP activity of DP MSCs on 14th and 21st days of osteogenic differentiation.

The mineralization indicator CaP deposition formed upon osteogenic induction was assessed by von Kossa staining. It showed that compared to undifferentiated cells, DP MSCs induced with osteogenic stimulants for 14 and 21 days have calcium depositions which were stained brown colour. The calcium deposition was clearly seen in MSCs induced for 21 day compared to cells induced for day 14 (Figure 19).

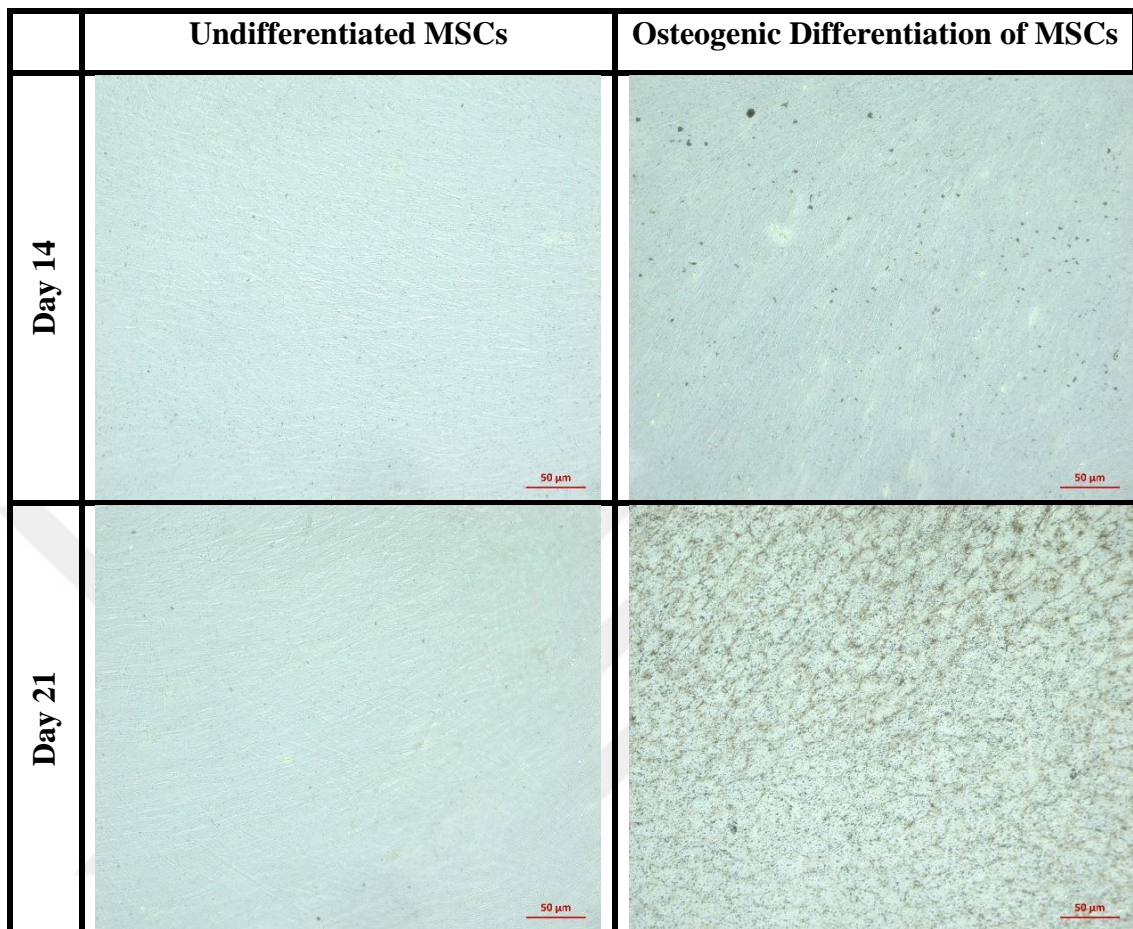


Figure 19. Light microscope images of DP MSCs induced to osteogenic differentiation and undifferentiated cells after von Kossa staining on days 14 and 21. Magnification: X20, scale bar: 50 μm .

4.2.1.5 Chondrogenic Differentiation of Dental Pulp MSCs

DP MSCs were cultured for 14 and 21 days in the chondrogenic induction medium, while the control was undifferentiated cells in the absence of induction. To demonstrate chondrogenic differentiation, the cells were stained with Alcian Blue for mucopolysaccharides. The number of synthesized polysaccharides seen in blue color

was increased on days 14 and 21 upon chondrogenic induction compared to undifferentiated cells' ECM (Figure 20).

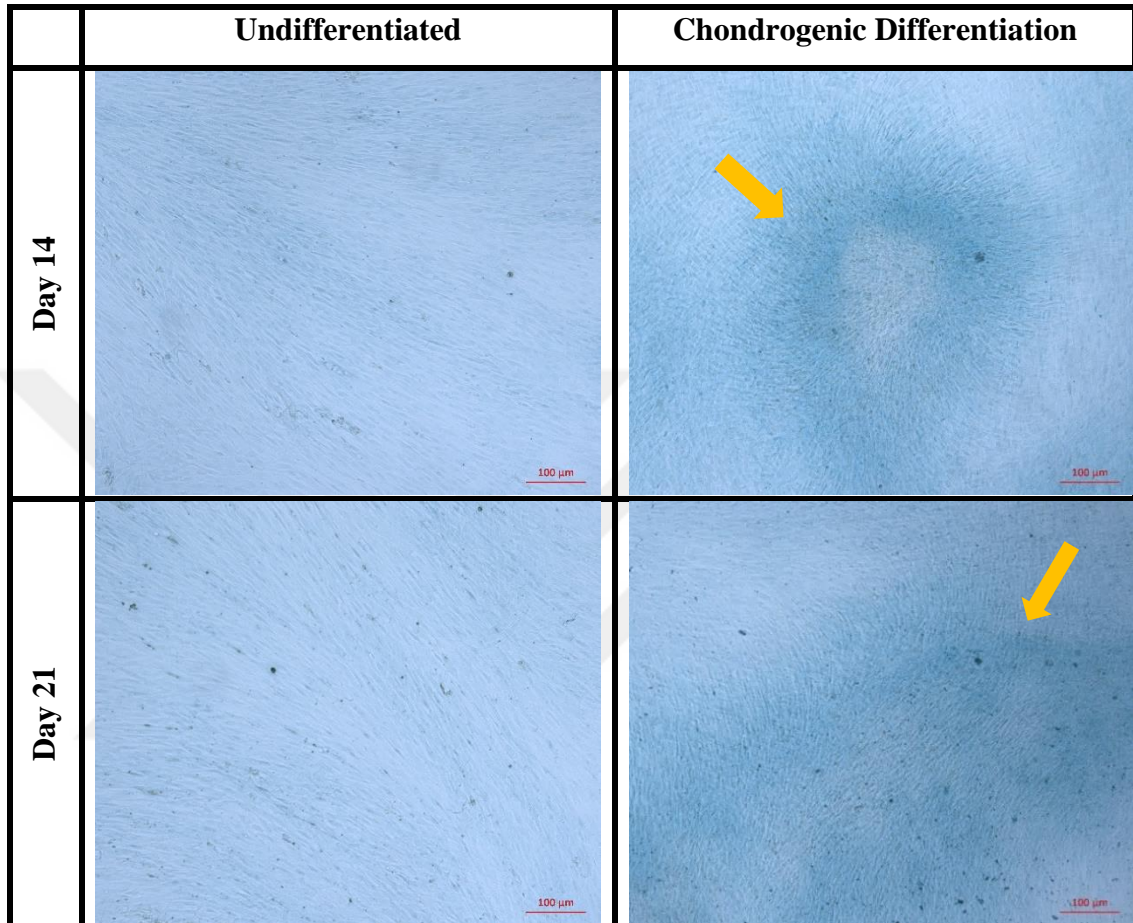


Figure 20. Light microscope images of DP MSCs in undifferentiated state and after chondrogenic induction on days 14 and 21 after Alcian Blue staining. Magnification: X10, scale bar: 100µm.

4.2.2 Tenogenic Differentiation of Dental Pulp MSCs

DP MSCs cultured for 14 days in tenogenic induction medium containing GDF7/BMP12 growth factor as the details given in Section 3.2.2.3. It was observed that DP MSCs induced for tenogenic differentiation significantly expressed tenocyte markers, scleraxis and tenomodulin compared to undifferentiated cells (Figure 21). The results showed the success of tenogenic induction medium which was used in the further studies.

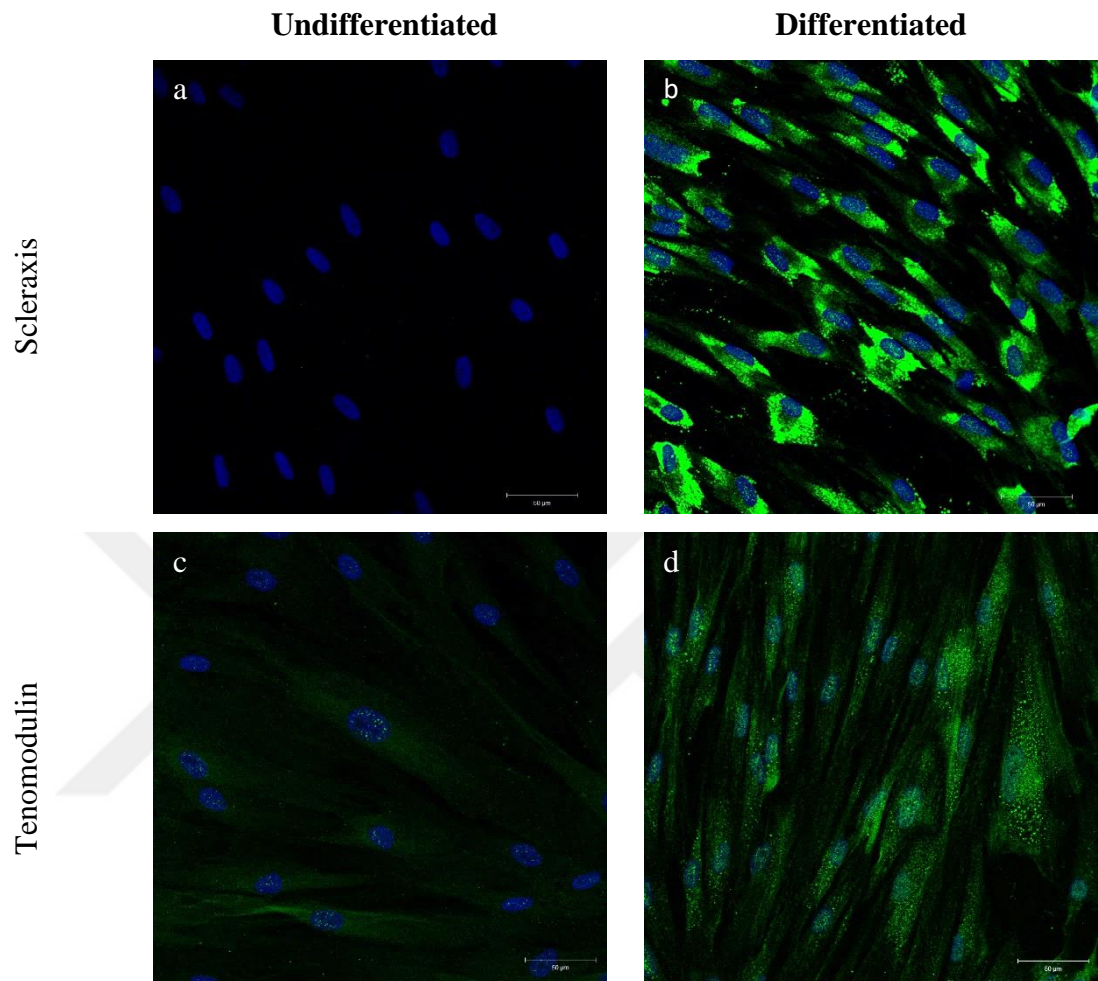


Figure 21. Confocal images of (a,c) undifferentiated DP MSCs and (b,d) DP MSCs cultured for 14 days in tenogenic induction medium. The expression of tenogenic markers, (a,b) scleraxis (green) and (c,d) tenomodulin (green) were shown by immunocytochemistry. The nucleus (blue) of the cells were counterstained with DAPI Magnification: 20X, scale bar: 50 μ m

4.2.3 Behaviour of Stem Cells on Electrospun Fibrous Mats

4.2.3.1 DP MSC Organization on the Scaffolds

Dental Pulp MSCs' organization and their alignment on the electrospun fibrous mats (without melatonin) were investigated by Phalloidin and DAPI staining for actin organization and nucleus, respectively. It was observed that DP MSCs realized the different topography of the random and aligned fibrous mats (Figure 22 and 23). DP MSCs were spread in all directions with random organization of actin filaments and round nuclei (Figure 22). It was observed that DP MSCs were well-oriented in anisotropic manner in the direction of fiber axis and their nuclei were elongated on the aligned fibrous mat (Figure 23).

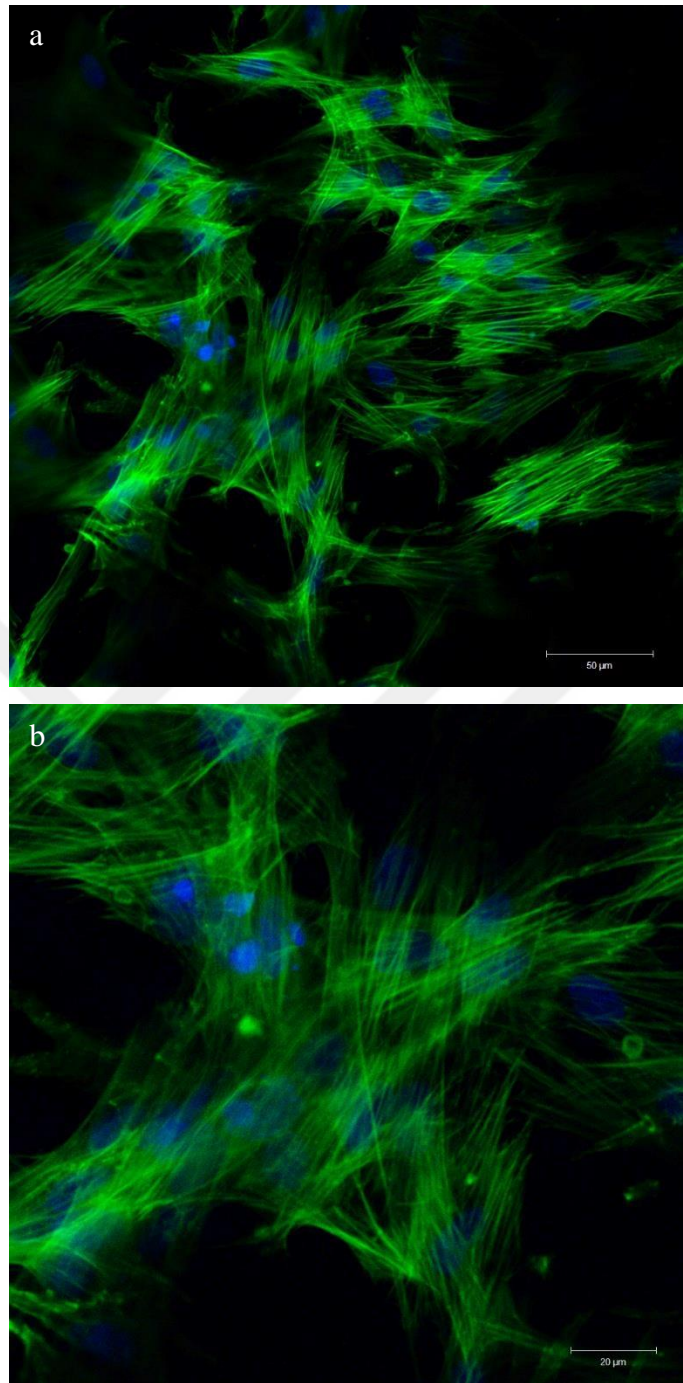


Figure 22. Confocal microscope images of DP MSCs on the random fibrous mat. The cells were stained with Phalloidin-DAPI for actin filaments (green) and nuclei (blue), respectively. Magnification: a) 20X, scale bar: 50 μm , b) 40X, scale bar: 20 μm .

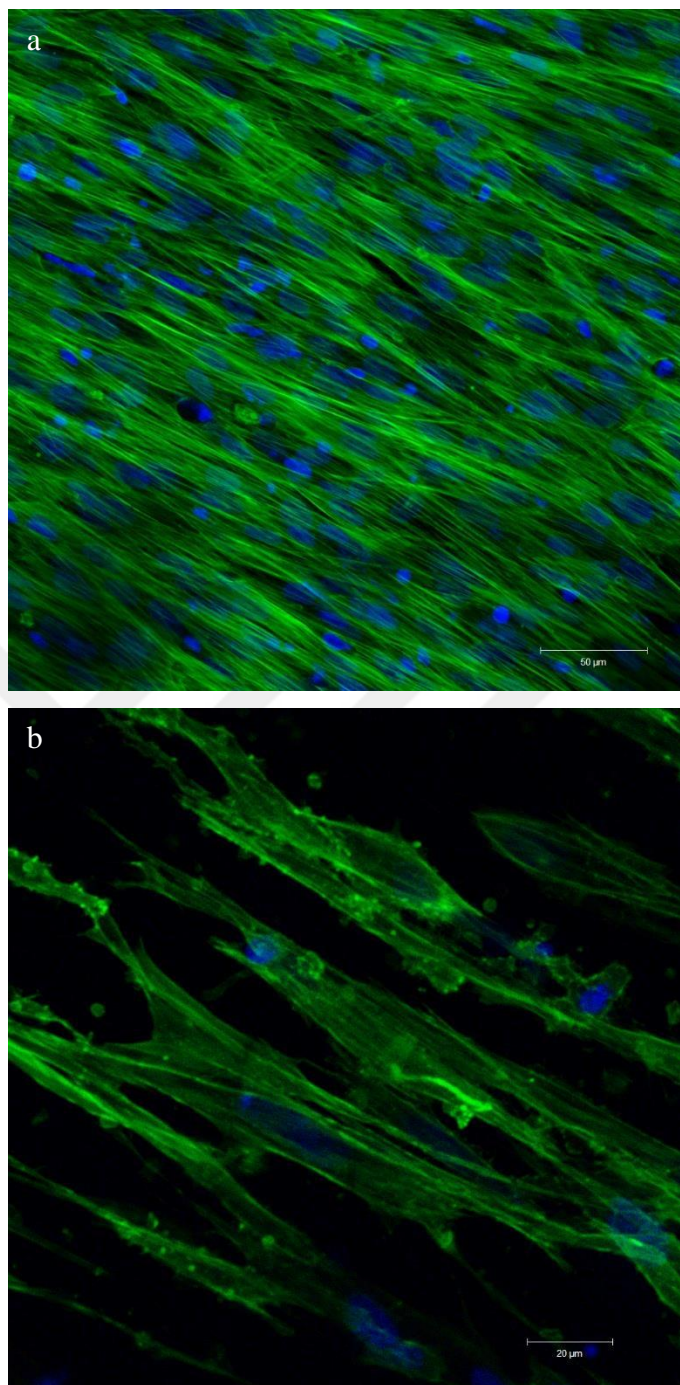


Figure 23. Confocal microscope images of DP MSCs on the aligned electrospun fibrous mat. The cells were stained with Phalloidin-DAPI for actin filaments (green) and nuclei (blue), respectively. Magnification: a) 20X, scale bar: 50 μm , b) 40X, scale bar: 20 μm .

4.2.3.2 Proliferation and Cell Activity of DP MSCs on the Scaffolds

The proliferation of cells on the aligned and random fibrous mats prepared with and without melatonin were determined by MTS assay. The cells on TCPS were used as control. DP MSCs were seeded on the mats at a density of 2×10^4 cells/sample. To evaluate cell attachment, MTS was done after one day of culture. The cell growth on these scaffolds were followed by conducting MTS assay on day 7,14 and 21.

The first day MTS results showed that the cells were attached onto both aligned and random fibrous mats whether the melatonin was present or not (Figure 24 and 25). The number of cells was increased by time on both aligned and random fibrous mat with or without melatonin. A significant increase in number of MSCs was determined on day 14 on both random and aligned electrospun mats with and without melatonin. This increase continued on day 21, except random fiber without melatonin group. The increase in cell number by time was significant, especially on the aligned fibrous mat as about five-fold on day 21 (Figure 24). The melatonin showed a relatively positive effect on cell proliferation with a slightly higher cell number in melatonin groups compared to without melatonin groups (Figure 24 and 25).

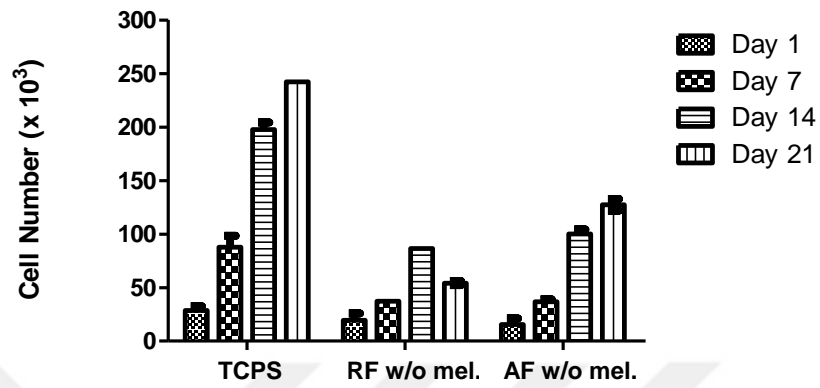


Figure 24. Proliferation of DP MSCs on P(L-D,L)LA-PLGA electrospun fibrous mats prepared in the absence of melatonin (without melatonin group).

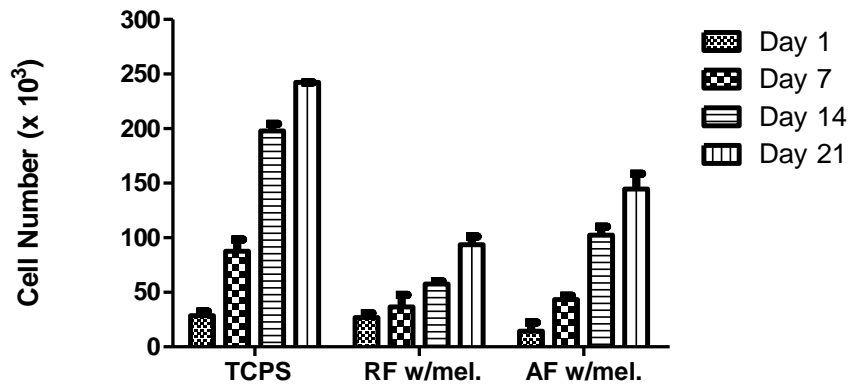


Figure 25. Proliferation of DP MSCs on P(L-D,L)LA-PLGA electrospun fibrous mat in the presence of melatonin (with melatonin group)

4.2.3.3 Evaluation of tenogenic differentiation of DP MSCs on the scaffolds by immunocytochemistry

The tenogenic induction DP MSCs to differentiate into tenocytes on the random and aligned electrospun fibrous mats prepared with and without melatonin was investigated by immunostaining against tenogenic markers, scleraxis and tenomodulin (Figures 26-33). Scleraxis (SCX), a member of the basic helix-loop-helix superfamily of transcription factors, is a one of the specific tendon marker. Tenomodulin (TNMD), a late differentiation marker of tenocyte, regulates tenocyte proliferation. These molecules play important roles in regulating the fate of tendon cells.

It was shown that the cells on the aligned and random fibrous mats were significantly expressed scleraxis (Figure 26-29). It was observed that the presence of melatonin did not affect the expression of scleraxis on both surfaces.

The other tenogenic marker tenomodulin (TNMD) expression was also seen by DP MSCs induced with tenogenic differentiation medium on both aligned and random fibrous mats (Figure 30-33). However, it was observed that tenomodulin expression of cells on both surfaces was slightly low in the presence of melatonin compared to the cells on scaffolds prepared without melatonin. In fact, the expression of tenogenic markers scleraxis and tenomodulin showed the differentiation of DP MSCs into tenocytes on both aligned and random fibrous mats. The immunocytochemistry and MTS results implied that the presence of melatonin within the scaffold slightly increased the proliferation while slightly lower their differentiation into tenocytes. This could be due to that the proliferation and differentiation processes were inversely proportional.

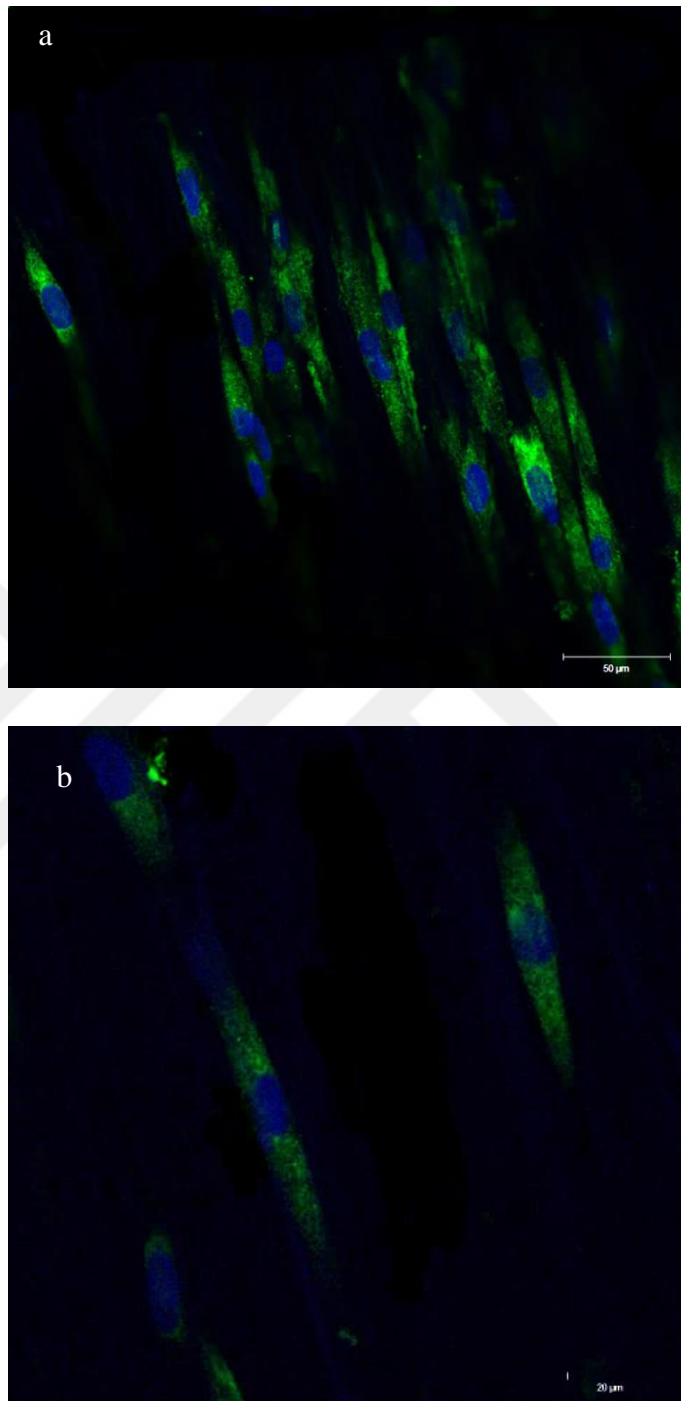


Figure 26. Confocal images of the cells on the aligned fibrous mat with melatonin at the end of 14 day of tenogenic induction. The cells were immunostained against scleraxis (green) and counterstained with DAPI for nucleus (blue). Magnifications: (a) X20, scale bar: 50 μ m, (b) X40, scale bar: 20 μ m.

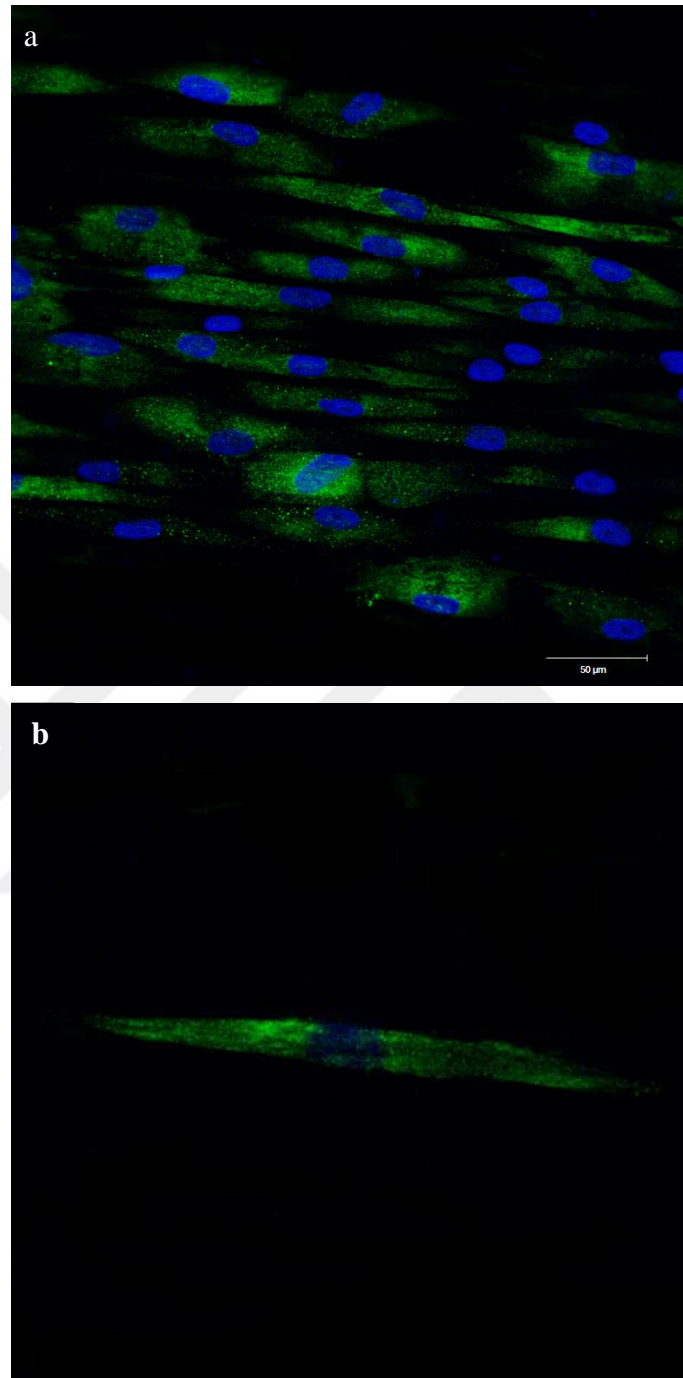


Figure 27. Confocal images of the cells on the aligned fibrous mat without melatonin at the end of 14 day of tenogenic induction. The cells were immunostained against scleraxis (green) and counterstained with DAPI for nucleus (blue). Magnifications: (a) X20, scale bar: 50 μ m, (b) X40, scale bar: 20 μ m.

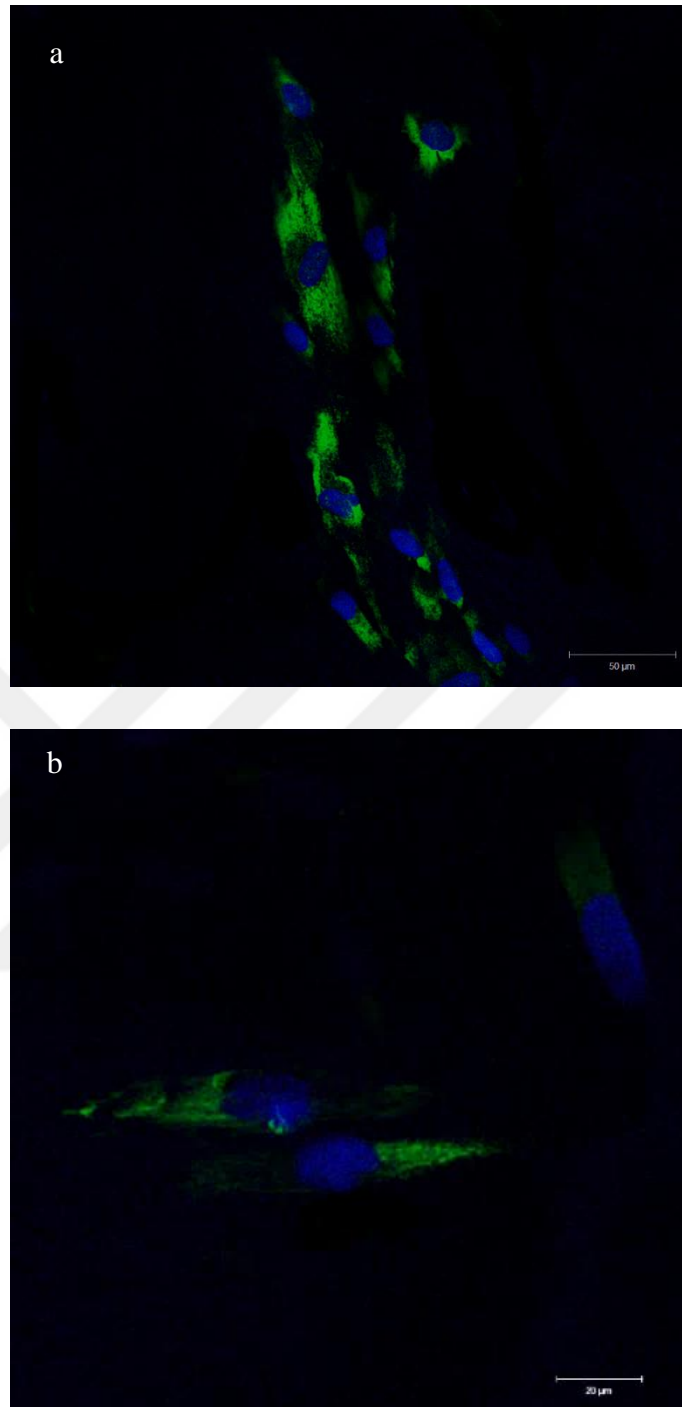


Figure 28. Confocal images of the cells on the random fibrous mat with melatonin at the end of 14 day of tenogenic induction. The cells were immunostained against scleraxis (green) and counterstained with DAPI for nucleus (blue). Magnifications: (a) X20, scale bar: 50μm, (b) X40, scale bar: 20μm

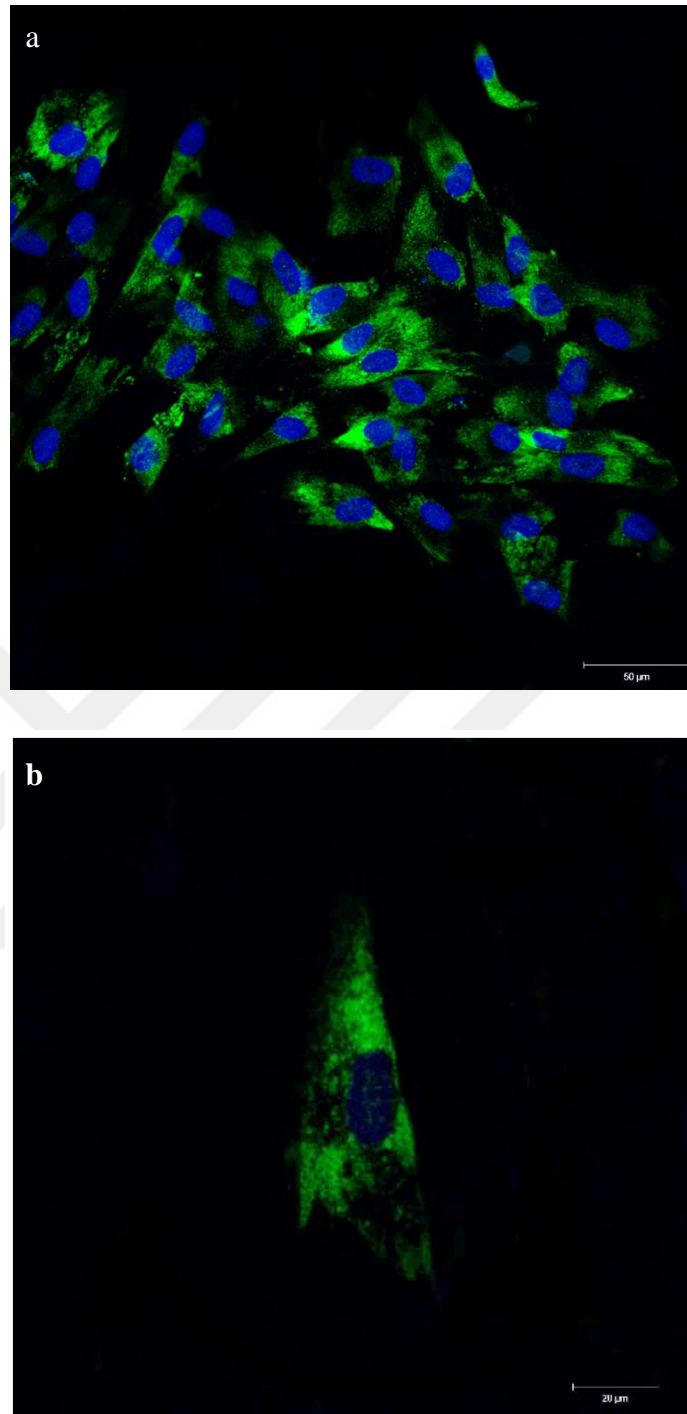


Figure 29. Confocal images of the cells on the random fibrous mat without melatonin at the end of 14 day of tenogenic induction. The cells were immunostained against scleraxis (green) and counterstained with DAPI for nucleus (blue). Magnifications: (a) X20, scale bar: 50μm, (b) X40, scale bar: 20μm.

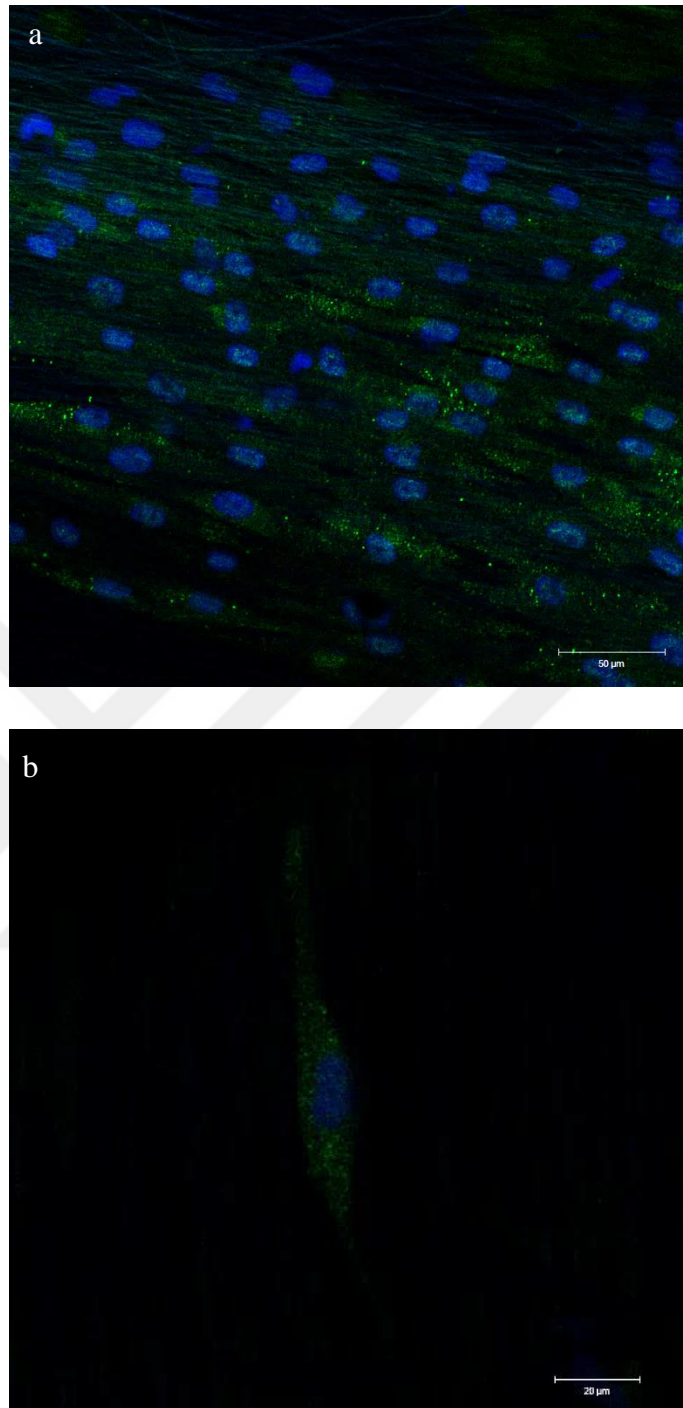


Figure 30. Confocal images of the cells on the aligned fibrous mat with melatonin at the end of 14 day of tenogenic induction. The cells were immunostained against tenomodulin (green) and counterstained with DAPI for nucleus (blue). Magnifications: (a) X20, scale bar: 50 μ m, (b) X40, scale bar: 20 μ m.

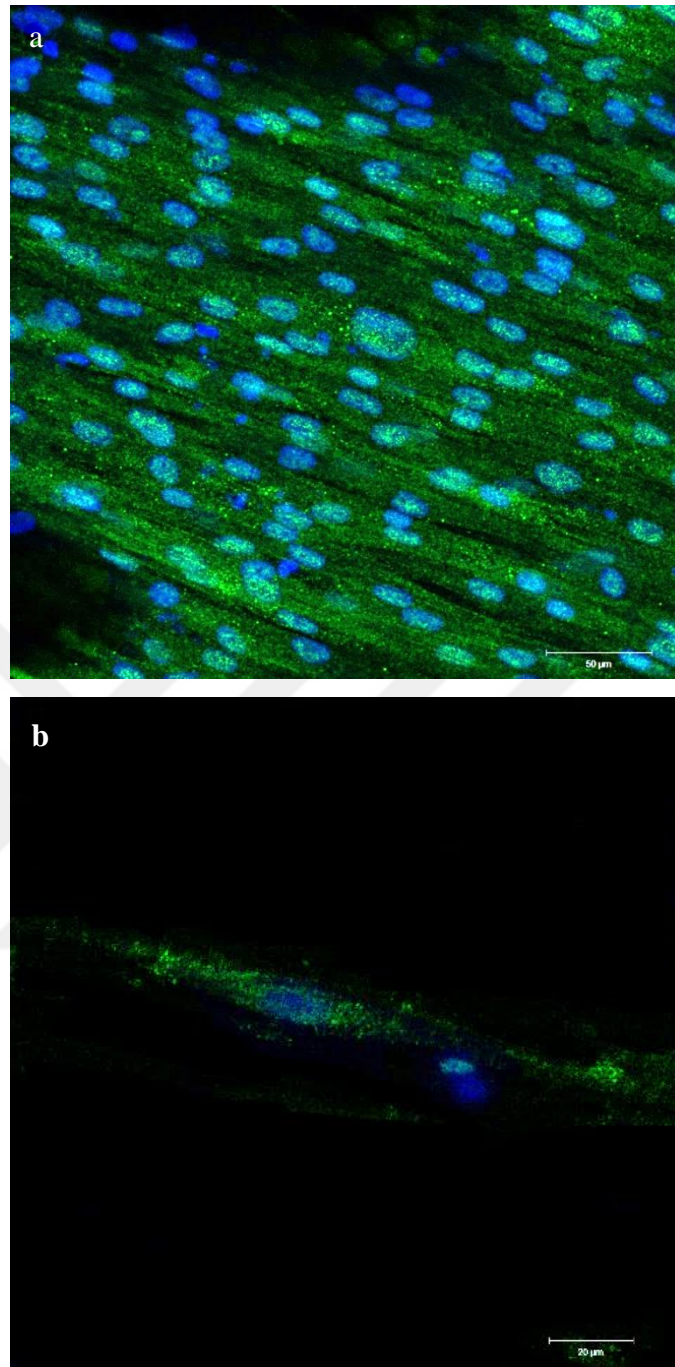


Figure 31. Confocal images of the cells on the aligned fibrous mat without melatonin at the end of 14 day of tenogenic induction. The cells were immunostained against tenomodulin (green) and counterstained with DAPI for nucleus (blue). Magnifications: (a) X20, scale bar: 50μm, (b) X40, scale bar: 20μm.

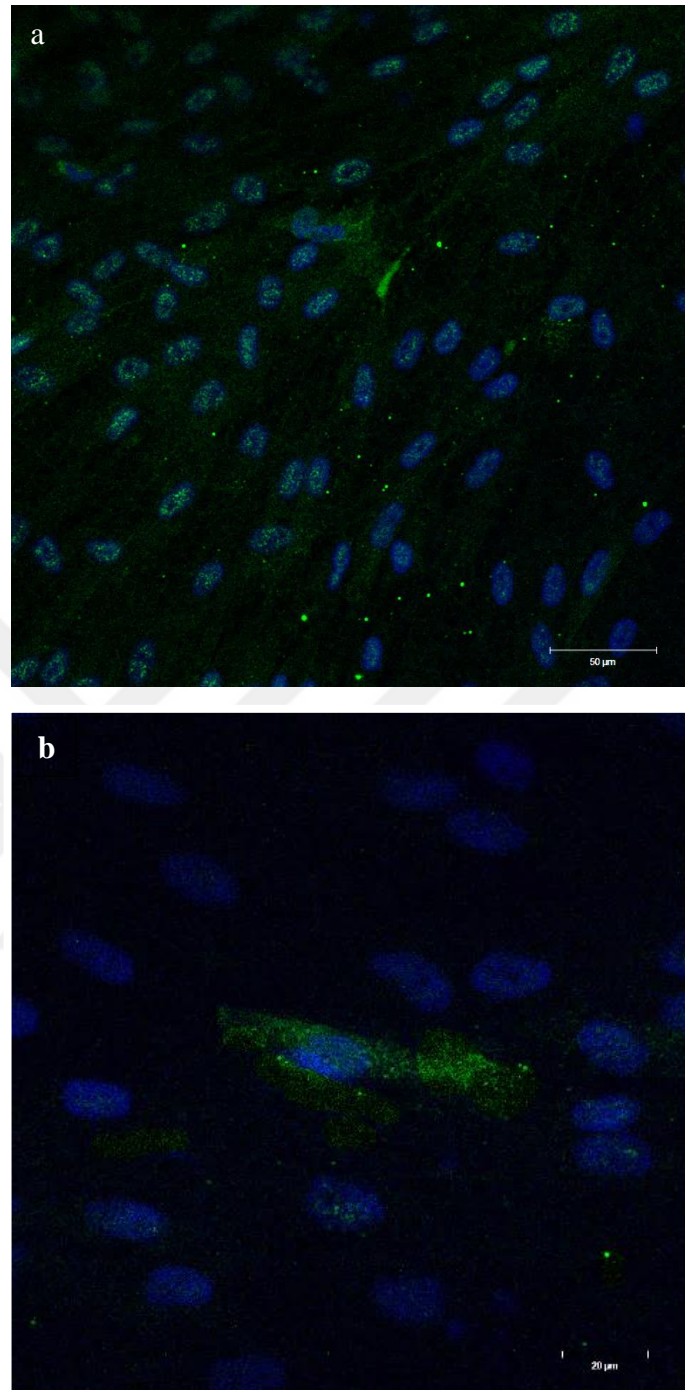


Figure 32. Confocal images of the cells on the random fibrous mat melatonin at the end of 14 day of tenogenic induction. The cells were immunostained against tenomodulin (green) and counterstained with DAPI for nucleus (blue). Magnifications: (a) X20, scale bar: 50 μ m, (b) X40, scale bar: 20 μ m.

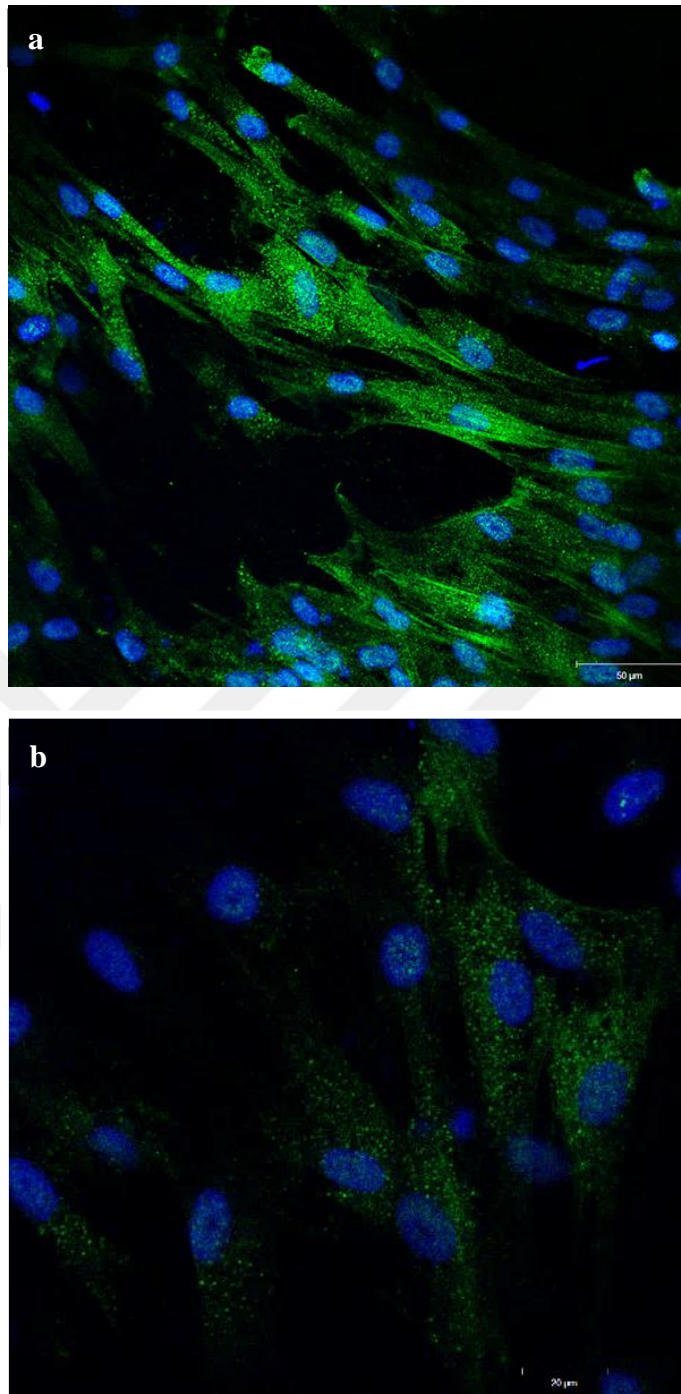


Figure 33. Confocal images of the cells on the random fibrous mat without melatonin at the end of 14 day of tenogenic induction. The cells were immunostained against tenomodulin (green) and counterstained with DAPI for nucleus (blue). Magnifications: (a) X20, scale bar: 50 μ m, (b) X40, scale bar: 20 μ m.

4. DISCUSSION AND CONCLUSION

Tendon tissue connects muscle to bone and its main role generates transmission of forces during joint movements (47). Because of overuse or age-related degeneration, tendon damages have become commonly seen clinical problem among musculoskeletal disorders. In the United States, about 17 million musculoskeletal injuries have been reported per year tendon and ligament injuries and one of the most injured tendons in the body is the Achilles tendon which causes long-term overuse and repetitive activities. Clinical cases reported that about 80% of tendon ruptures occurred during sporting activities (48,49,50,51).

Tendon is composed of dense regular connective tissue with parallel and closely packed collagen fibres and its cells. It has a well-organized ECM architecture and guided cells (48,52,53). Tendon healing process includes tendon cells and their surrounding ECM. After tendon injury, scar formation and tissue repair occur in three stages: tissue inflammation, cell proliferation, and ECM remodelling. Tendon healing is composed of two mechanisms: extrinsic and intrinsic healing. Extrinsic healing includes the invasion of inflammatory cells to the injury site, synthesis of the collagen matrix and enhancement of the repair process. On the other hand, intrinsic healing includes local stem/progenitor cells (49, 54). Secretion of inflammatory cytokines support the tendon healing process such as interleukin-6 and interleukin-1 β (55). Matrix remodelling is known as a slow, continuous process which includes proteoglycans and collagens (56,57). Additionally, several growth factors are released by cells located at the injury site, to ensure repair of tendon damages. For instance, TGF- β , IGF-1, PDGF, bFGF, VEGF and bone morphogenetic proteins (BMP) are involved in different phases of healing process (49,54). The members of the TGF- β superfamily is GDF family (GDF-5/BMP-14, GDF-6/BMP-13, and GDF-7/BMP-12). Besides

generally associated with chondrogenic and osteogenic functions, BMPs are potential factors to be used in tenogenic differentiation (58,59).

Since BMP/GDF are involved in tendon repair, it was used in this study to differentiate DP MSCs into tenogenic cells. It has been reported that GDF-7/BMP-12 promotes tendon repair. Fu et al., showed that GDF-7/BMP-12 stimulated the proliferation and matrix production of human patellar tendon fibroblasts (60). In another study, it was reported that GDF-7/BMP-12 induced BMSCs into tenocytes *in vitro* and this differentiation was shown by mRNA expression of tenomodulin and decorin (61). In addition, it was revealed that treatment of hASCs with BMP-12 might affect proliferation and migration capacity, secretory activity, and immunomodulatory properties of the cells (62).

Take into consideration the natural healing process, in this tissue engineering study it was aimed to develop well-organized scaffold with aligned cells to mimic architecture of tendon tissue. In addition, melatonin was integrated into scaffold to enhance collagen synthesis which is required for tendon healing. Moreover, melatonin plays important role in pain modulation and it has anti-inflammatory effect (45). Therefore, melatonin has been used in regenerative medicine studies.

In tendon-to-bone healing models it was reported that melatonin-loaded PCL membranes promoted chondrogenic differentiation of human bone marrow-derived mesenchymal stem cells (hBMSCs) under *in vitro* conditions (46). In another study, the melatonin loaded PLGA micropatterned scaffolds were developed to support tendon regeneration. In this way, some vital properties such as drug-release behaviour, cell biological features and cell alignment have been investigated (63).

In conclusion, the synergistic effects of the topography guided platform and the bioactive agent expect to make this construct an ideal guided scaffold to be used in tendon tissue engineering. This tissue engineered tendon including stem cells would be a potential therapeutic approach for patient specific treatments in regenerative medicine.



6. REFERENCES

1. Kannus, P. Structure of the tendon connective tissue. *Scand J Med Sci Sports*. 2000; 10: 312–320.
2. Jeffrey H. Weinreb, Chirag Sheth, Chirag Sheth, et.al. Tendon structure, disease, and imaging. *Muscles, Ligaments and Tendons Journal*. 2014; 1: 66-73.
3. R J Hodgson, P J O'Connor , et.al. Tendon and ligament imaging. *The British Journal of Radiology*. 2012; 1157–1172.
4. Geoffroy Nourissat, Francis Berenbaum and Delphine Duprez. Tendon injury: from biology to tendon repair. *Nature Reviews Rheumatology*.2015;1, 223–233.
5. Bruno Magnan, Manuel Bondi, Silvia Pierantoni,Elena Samaila.The pathogenesis of Achilles tendinopathy. *Foot and Ankle Surgery* , 2014; 154–159
6. Riley Graham.Chronic tendon pathology: molecular basis and therapeutic implications.*Expert Reviews in Molecular Medicine* , 2005;7(5):1-25.
7. Sebastian A. Muller, Atanas Todorov, Patricia E. Heisterbach,Ivan Martin and Martin Majewski.Tendon healing: an overview of physiology, biology, and pathology of tendon healing and systematic review of state of the art in tendon bioengineering. *Knee Surg Sports Traumatol Arthrosc*. 2015; 2097–2105.
8. Gloria R. Sue, James Chang. Tendon Repair.*Global Reconstructive Surgery*. 2020; 145 (2): 471–81.
9. Mark F. Pittenger, Dennis E. Discher, Bruno M. Péault, Donald G. Phinney, Joshua M. Hare & Arnold I. Caplan. Mesenchymal stem cell perspective: cell biology to clinical progress. *npj Regenerative Medicine*. 2019; 4,(22).
10. R Langer, J P Vacanti. Tissue Engineering. *Science*. 1993; 260(5110):920-6.
11. Hampson et al. Tendon Tissue Engineering.*Topics in Tissue Engineering*. 2008; Vol. 4.
12. Wojciech Zakrzewski, Maciej Dobrzyński,Maria Szymonowicz,Zbigniew Rybak. Stem cells: past, present, and future. *Stem Cell Research & Therapy*. 2019;10:68 .
13. Imran Ullah, Raghavendra Baregundi Subbarao,and Gyu Jin Rho. Human mesenchymal stem cells - current trends and future prospective. *Biosci Rep.*, 2015; 35(2): e00191.
14. Sylvestar Darvin Sandhaanam, Ganesan Pathalam, Sudarsanam Dorairaj, Vincent Savariar. Mesenchymal stem cells (MSC): Identification, Proliferation and Differentiation – A Review Article. *PeerJ PrePrints*. 2013; 1:e148v1.

15. Imran Ullah, Raghavendra Baregundi Subbarao and Gyu Jin Rho. Human mesenchymal stem cells - current trends and future prospective. *Biosci. Rep.*, 2015; 28;35(2):e00191.
16. Wagner, W., Wein, F., Seckinger, A., Frankhauser, M., Wirkner, U., Krause, U., Blake, J., Schwager, C., Eckstein, V., Ansorge, W. and Ho, A.D. Comparative characteristics of mesenchymal stem cells from human bone marrow, adipose tissue, and umbilical cord blood. *Exp. Hematol.* 2005; 33(11):1402-16.
17. Raynaud, C.M., Maleki, M., Lis, R., Ahmed, B., Al-Azwani, I., Malek, J., Safadi, F.F. and Rafii, A. Comprehensive characterization of mesenchymal stem cells from human placenta and fetal membrane and their response to osteoactivin stimulation. *Stem Cells Int.* 2012;658356.
18. Cai, J., Li, W., Su, H., Qin, D., Yang, J., Zhu, F., Xu, J., He, W., Guo, X., Labuda, K. et al. Generation of human induced pluripotent stem cells from umbilical cord matrix and amniotic membrane mesenchymal cells. *J. Biol. Chem.* 2010; 9;285(15):11227-34
19. In 't Anker, P.S., Scherjon, S.A., Kleijburg-van der Keur, C., Noort, W.A., Claas, F.H., Willemze, R., Fibbe, W.E. and Kanhai, H.H. Amniotic fluid as a novel source of mesenchymal stem cells for therapeutic transplantation. *Blood.* 2003;15;102(4):1548-9.
20. Huang, G.T., Gronthos, S. and Shi, S. Mesenchymal stem cells derived from dental tissues vs. those from other sources: their biology and role in regenerative medicine. *J. Dent. Res.* 2009;88(9):792-806.
21. Rezacova, M. The response of human ectomesenchymal dental pulp stem cells to cisplatin treatment. *Int. Endod. J.* 2012;45(5):401-12.
22. Y Isobe 1, N Koyama 2, K Nakao 1 and et al. Comparison of human mesenchymal stem cells derived from bone marrow, synovial fluid, adult dental pulp, and exfoliated deciduous tooth pulp. *Int J Oral Maxillofac Surg.*2016 45(1):124-31.
23. Maacha S. et.al, Paracrine Mechanisms of Mesenchymal Stromal Cells in Angiogenesis. *Hindawi Stem Cells International.*2020;4356359.
24. Yu Han, Xuezhou Li, Yanbo Zhang, Yuping Han, Fei Chang and Jianxun Ding. Mesenchymal Stem Cells for Regenerative Medicine. *Cells.*2019; 13;8(8):886.
25. Ramalingam Murugan, Seeram Ramakrishna. Design Strategies of Tissue Engineering Scaffolds With Controlled Fiber Orientation. *Tissue Engineering.*2007; 13(8):1845-66.
26. Murugan, R., and Ramakrishna, S. Bioactive nanomaterials in bone grafting and tissue engineering. *Composites Science and Technology.*2005; 65(15-16):2385-2406
27. Umile Giuseppe Longo, Alfredo Lamberti, Stefano Petrillo. Scaffolds in Tendon Tissue Engineering. *Stem Cells International.* .2012;(5):517165

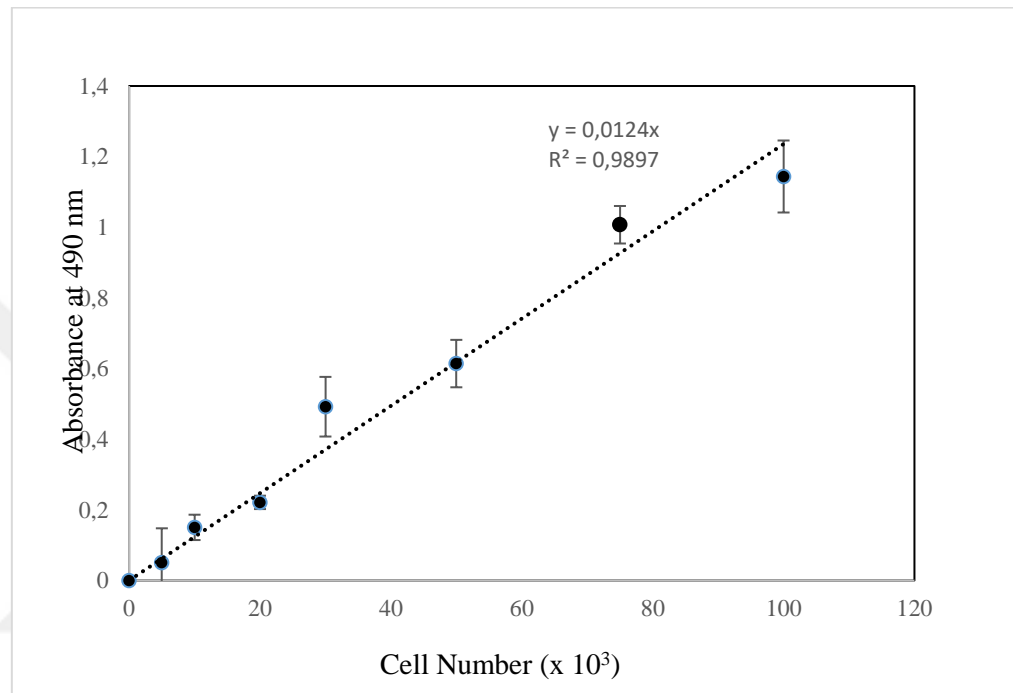
28. U. G. Longo, A. Lamberti, G. Rizzello, N. Maffulli, and V. Denaro. Synthetic augmentation in massive rotator cuff. *Medicine and Sport Science*. 2012; vol 57, pp 168–177.
29. Murugan, R., and Ramakrishna, S. Nano-featured scaffolds for tissue engineering: a review of spinning methodologies. *Tissue Eng.* 2006; 12(3):435-47.
30. U. G. Longo, E. Franceschetti, S. Petrillo, N. Maffulli. Latissimus dorsi tendon transfer for massive irreparable rotator cuff tears: a systematic review. *SportsMed Arthrosc.* 2011; 428–437.
31. B. P. Chan, K. W. Leong. Scaffolding in tissue engineering: general approaches and tissue-specific considerations. *Eur Spine J.* 2008;S467–S479.
32. J. Chen, J. Xu, A. Wang, and M. Zheng . Scaffolds for tendon and ligament repair: review of the efficacy of commercial products. *Expert Review of Medical Devices.* 2009; 6(1):61-73
33. Webb, A.R., Yang, J., and Ameer, G.A. Biodegradable polyester elastomers in tissue engineering. *Expert Opin. Biol. Ther.* 2004; 4(6):801-12.
34. Wuisman, P. I. J. M. Bioresorbable polymers: heading for a new generation of spinal cages. *Eur Spine J.* 2006; 15(2): 133–148.
35. S. G. Sclamberg, J. E. Tibone, J.M. Itamura, and S. Kasraeian. Six-month magnetic resonance imaging follow-up of large and massive rotator cuff repairs reinforced with porcine small intestinal submucosa. *Journal of Shoulder and Elbow Surgery.* 2004;13(5):538-41.
36. M. H. Zheng, J. Chen, Y. Kirilak, C. Willers, J. Xu, and D. Wood. Porcine small intestine submucosa (SIS) is not an acellular collagenous matrix and contains porcine DNA: possible implications in human implantation. *Journal of Biomedical Materials Research B.* 2005; 73(1):61-7
37. H. W. Ouyang, T. Cao, X. H. Zou et al. Mesenchymal stem cell sheets revitalize nonviable dense grafts: Implications for repair of large-bone and tendon defects. *Transplantation.* 2006; 82(2):170-4
38. Piergiorgio Gentile, Valeria Chiono, Irene Carmagnola. An Overview of Poly(lactic-co-glycolic) Acid (PLGA)-Based Biomaterials for Bone Tissue Engineering. *Int. J. Mol. Sci.* 2014; 28;15(3):3640-59.
39. Han, Yang Wu and Yi. 3D functional scaffolds for tendon tissue engineering. *Functional 3D Tissue Engineering Scaffolds.* 2018;Chapter 15.
40. Murugan, R., and Ramakrishna, S. Nanostructured biomaterials. *Encyclopedia of Nanoscience and Nanotechnology.* California: American Scientific Publishers. 2004;595–613. *Foot Ankle Int.* 2008; 29(7):671-6.

41. Pham, Q.P., Sharma, U., and Mikos. Electrospinning of polymeric nanofibers for tissue engineering applications: a review. *Tissue Eng.*2006; 12(5):1197-211.
42. Kim HN, Jiao A, Hwang NS, Kim MS, Kang DH, Kim DH, Suh KY. Nanotopography-guided tissue engineering and regenerative medicine.*Advanced Drug Delivery Reviews.* 2012; 65(4):536-558.
43. P. Fratzl, K. Misof, I. Zizak, G. Rapp, H. Amenitsch, S. Bernstorff. Fibrillar structure and mechanical properties of collagen. *J. Struct. Biol.*1998; SB983966
44. A.M. Cribb, J.E. Scott. Tendon response to tensile-stress — an ultrastructural investigation of collagen–proteoglycan interactions in stressed tendon. *J. Anat.* 1995; 187(Pt 2): 423–428.
45. Ambriz-Tututi M, Rocha-González HI, Cruz SL, Granados-Soto V. Melatonin: a hormone that modulates pain. *Life Sciences.* 2009; (15-16):489-498.
46. Wei Song, Zhijie Ma, Chongyang Wang, Haiyan Li and Yaohua He. Pro-chondrogenic and immunomodulatory melatonin-loaded electrospun membranes for tendon-to-bone healing. *J. Mater. Chem. B.*2019;14;7(42):6564-6575.
47. Sharma P, Maffulli N. Tendinopathy and tendon injury: the future. *Disabil Rehabil.* 2008;30:1733-1745.
48. Józsa L, Lehto MU, Järvinen M, et al. A comparative study of methods for demonstration and quantification of capillaries in skeletal muscle. *Acta Histochemica.*1993;94:89-96.
49. James R, Kesturu G, Balian G, Chhabra AB. Tendon: biology, biomechanics, repair, growth factors, and evolving treatment options. *J Hand Surg Am* 2008; 33(1):102-12.
50. M., Kvist. Achilles tendon injuries in athletes. *Sports Med.* 1994;18:173-201.
51. Heckman DS, Gluck GS, Parekh SG. Tendon disorders of the foot and ankle, part 2: Achilles tendon disorders.*Am J Sports Med.*2009; 37(6):1223-34.
52. Fukuta S, Oyama M, Kavalkovich K, Fu FH, Niyibizi C. Identification of types II, IX and X collagens at the insertion site of the bovine achilles tendon. *Matrix Biol.*1998;17:65-73.
53. Fukushige T, Kanekura T, Ohuchi E, Shinya T, Kanzaki T. Immunohistochemical studies comparing the localization of type XV collagen in normal human skin and skin tumors with that of type IV collagen. *J Dermatol.*2005; 32(2):74-83.
54. Kajikawa Y, Morihara T, Sakamoto H, et al. Platelet-rich plasma enhances the initial mobilization of circulation-derived cells for tendon healing. *J Cellular Physiol.*2008; 215(3):837-45.

55. Sharma P, Maffulli N. Tendon injury and tendinopathy: healing and repair. *J Bone Joint Surg [Am]*. 2005; 87(1):187-202.
56. Karsten Knobloch, Uzung Yoon, Peter M Vogt. Acute and Overuse Injuries Correlated to Hours of Training in Master Running Athletes. *Foot Ankle Int*.2008; 29(7):671-6.
57. Kong D, Xu L, Yu Y, et al. Regulation of Ca²⁺-induced permeability transition by Bcl-2 is antagonized by Drp1 and hFis1. *Molecular and Cellular Biochemistry*.2005; 272: 187–199.
58. Eliasson P, Fahlgren A, Aspenberg P. Mechanical load and BMP signaling during tendon repair: a role for follistatin? *Clin Orthop Relat Res*. 2008; 466(7): 1592–1597.
59. P. P. Y. Lui, Y. F. Rui, M. Ni and K. M. Chan. Tenogenic differentiation of stem cells for tendon repair – what is the current evidence? *J Tissue Eng Regen Med*. 2011; 5(8):e144-63.
60. Weronika Zarychta-Wiśniewska Anna Burdzinska et al. Bmp-12 activates tenogenic pathway in human adipose stem cells and affects their immunomodulatory and secretory properties. *BMC Cell Biology*. 2017;18: 13.
61. Stefania Violini, Paola Ramelli, Laura F Pisani, Chiara Gorni et al,. Horse bone marrow mesenchymal stem cells express embryo stem cell markers and show the ability for tenogenic differentiation by in vitro exposure to BMP-12. *BMC Cell Biology*. 2009; 10(1):29.
62. Sai Chuen Fu 1, Yim Ping Wong, Barbara Pui Chan, Hon Man Pau, Yau Chuk Cheuk, Kwong Man Lee, Kai-Ming Chan. The Roles of Bone Morphogenetic Protein (BMP) 12 in Stimulating the Proliferation and Matrix Production of Human Patellar Tendon Fibroblasts. *Life Sci*. 2003;16;72(26).
63. Xuetao Shi, Yihua Zhao et. al,. One-Step Generation of Engineered Drug-Laden Poly(lactic-co-glycolic acid) Micropatterned with Teflon Chips for Potential Application in Tendon Restoration. *ACS Applied Materials & Interfaces*. 2013; 5(21)
64. <http://sci.amegroups.com/article/viewFile/27241/html/168687>

7. APPENDICIES

Appendix 1. Calibration curve of human dental pulp mesenchymal stem cells at passage 3



Appendix 2. Ethical approval for the use of human DP MSCs



SAYI: ATADEK-2018/6
KONU: Etik Kurul Kararı

Sayın Dr. Öğr. Üyesi Deniz Yücel

Sorumluluğunu yürüttüğünüz **“Yönlü Platformlar ve Mezenkimal Kök Hücreler Kullanarak Tendon Doku Mühendisliği Yaklaşımı (Tendon Tissue Engineering Approach Using Guided Platforms and Mesenchymal Stem Cells)”** başlıklı proje 19.04.2018 tarih 2018/6 Sayılı Atadek Toplantısında görüşülmüş olup 2018-6/3 karar numarası ile tıbbi etik yönden uygun bulunmuştur.

Prof. Dr. Güldal SÜYEN
ATADEK Başkan Yardımcısı

Appendix 3. Ethical approval for the use of human DP MSCs (Continued Appendix 2)

**ACIBADEM MEHMET ALİ AYDINLAR ÜNİVERSİTESİ
TIBBİ ARAŞTIRMALAR DEĞERLENDİRME KURULU (ATADEK)**

Etik onay istenen tıbbi araştırmanın başlığı:

Yönlü Platformlar ve Mezenkimal Kök Hücreler Kullanarak Tendon Doku Mühendisliği Yaklaşımı
(Tendon Tissue Engineering Approach Using Guided Platforms and Mesenchymal Stem Cells)

Etik onay istenen tıbbi araştırmanın yürütücüsü (sorumlusu):

Dr. Öğr. Üyesi Deniz Yücel

Karar:

Kabul (Etik olarak uygun) (X) **Revizyon ()*** **Etik olarak uygun değil ()****

Toplantı Tarihi:19.04.2018

Karar Numarası: 2018-6/3

Kurul Üyesi-Unvan Ad-Soyad	İmza	Karara	
		Katılıyorum	Katılmıyorum***
Prof. Dr. İsmail Hakkı Ulus (Başkan)		()	()
Prof. Dr. Güldal Süyen (Başkan Yrd)		(X)	()
Prof.Dr. Mert Ülgen		(X)	()
Prof.Dr. Ükke Karabacak		(X)	()
Prof.Dr. A.Elif Eroğlu Büyüköner		()	()
Doç.Dr. Berrin Karadağ		(X)	()
Doç.Dr. Günseli Bozdoğan		()	()
Yrd.Doç.Dr. Fatih Artvinli		(X)	()

CURRICULUM VITAE

Personal Information

Name	Tuğçe	Surname	Deveci
Birth Place	Istanbul	Birth Date	20/09/1993
Nationality	Turkish	Phone Number	+90 539 6881618
E-mail	tugcedeveci.93@gmail.com		

Education

	Institution	Graduation Year
BSc	Istanbul University Biology Department	2015
High School	Kağıthane High School	2011

Experience

Job Title	Institution	Duration
ERASMUS+ Intern	Istituto Ortopedico Rizzoli The laboratory of Orthopaedic Pathology and Osteoarticular Tissue Regeneration BOLOGNA/ITALY	October-December 2018
Visiting researcher	Middle East Technical University- Center of Excellence in Biomaterials and Tissue engineering ANKARA/TURKEY	August, 2018
Laboratory Intern	Koç University Department of Reproduction Biology ISTANBUL/TURKEY	June 2016-February 2017

Languages	Reading	Speaking	Writing
English	Advanced	Advanced	Advanced

Foreign Language Examination Grade									
KPDS	ÜDS	IELTS	TOEFL IBT	TOEFL PBT	TOEFL CBT	FCE	CAE	CPE	YDS
									57.5

	Quantitative	Equally Weighted	Verbal
ALES Note	67,01958	67,23863	63,59500

Computer Skills

Program	Skill Degree
Microsoft Office	Very Good
GraphPad Prism	Good
Adobe Photoshop CS6	Intermediate

Presentations

Deveci T., Vasif Hasırcı., Yucel D. Tendon Tissue Engineering Using Dental Pulp Mesenchymal Stem Cells on Micropatterned Polymeric Films. 23rd Biomedical Science and Technology Symposium. 2019 (Poster Presentation).

Deveci T., Aksu U. Safety of Energy Drinks and Common Negative Effects. 21st National Congress of Biology Students. 2014 (Oral Presentation).